5-15-2020

Shuxuening injection facilitates neurofunctional recovery via down-regulation of G-CSF-mediated granulocyte adhesion and diapedesis pathway in a subacute stroke mouse model

Zhixiong Li
Tianjin University of Traditional Chinese Medicine

Guangxu Xiao
Tianjin University of Traditional Chinese Medicine

Ming Lyu
Tianjin University of Traditional Chinese Medicine

Yule Wang
Tianjin University of Traditional Chinese Medicine

Shuang He
Tianjin University of Traditional Chinese Medicine

See next page for additional authors

Biomedicine & Pharmacotherapy 127 (2020) 110213

Contents lists available at ScienceDirect

Biomedicine & Pharmacotherapy

journal homepage: www.elsevier.com/locate/biopha

Shuxuening injection facilitates neurofunctional recovery via down-regulation of G-CSF-mediated granulocyte adhesion and diapedesis pathway in a subacute stroke mouse model

Zhixiong Li[a,b,1], Guangxu Xiao[a,b,1], Ming Lyu[a,b,c], Yule Wang[a,b], Shuang He[a,b], Hongxia Du[a,b], Xintong Wang[a,b], Yuxin Feng[a,b], Yan Zhu[a,b,*]

[a] State Key Laboratory of Component-based Chinese Medicine, Tianjin University of Traditional Chinese Medicine, Beihua South Road, JingHai District, Tianjin, 301617, China
[b] Research and Development Center of TCM, Tianjin International Joint Academy of Biotechnology & Medicine, 220 Dongting Road, TEDA, Tianjin, 300457, China
[c] Institute of Chinese Materia Medica, China Academy of Chinese Medical Sciences, Beijing, 100700, China

ARTICLE INFO

Keywords:
Shuxuening injection
Subacute stroke
Cerebral ischemia-reperfusion injury
Neurofunctional recovery
Granulocyte adhesion and diapedesis
G-CSF

ABSTRACT

Post-stroke neural damage is a serious health concern which does not yet have an effective treatment. We have shown previously that Shuxuening injection (SXNI), a Ginkgo biloba extract-based natural medicine, protects brain after an acute ischemic stroke, but its efficacy for post-stroke recovery is not known. This study was to investigate whether SXNI can improve the prognosis of stroke at a subacute phase. Mice with cerebral ischemia-reperfusion injury (CIRI) were established by middle cerebral artery occlusion (MCAO), and drugs or saline were injected by the tail vein every 12 h after reperfusion. The therapeutic effect of SXNI was evaluated by survival rate, modified neurologic severity scores (mNSS), open-field test, locomotive gait patterns, cerebral infarction volume, brain edema and histopathological changes. Subsequently, a combined method of RNA-seq and Ingenuity® Pathway Analysis (IPA) was performed to identify key targets and pathways of SXNI facilitating the prognosis of stroke in mouse brain. The results of the transcriptome analysis were verified by real time reverse transcription-polymerase chain reaction (RT-PCR), enzyme-linked immunosorbent assay (ELISA), western blot (WB) and immunohistochemistry (IHC). The experimental results showed that in the new subacute stroke model, SXNI markedly improves the survival rate, neurological and motor functions and histopathological changes, and significantly reduces cerebral infarction and edema volume. RNA-seq analysis of subacute stroke mice with or without SXNI (3 mL/kg) indicated 963 differentially expressed genes (DEGs) with a fold change ≥ 1.5 and a P-value ≤ 0.01. IPA analysis of DEGs showed that granulocyte adhesion and diapedesis ranked first in the pathway ranking, and the most critical gene regulated by SXNI was *G-csf*. Simultaneously, RT-PCR, ELISA, WB and IHC results demonstrated that SXNI not only obviously reduced the mRNA expression levels of key genes *G-csf*, *Sele* and *Mac-1* in this pathway, but also significantly decreased the protein expression levels of G-CSF in serum and E-selectin and MAC-1 in brain tissues. In summary, our research suggested that SXNI can exert a remarkable neurofunctional therapeutic effect on stroke mice via down-regulating G-CSF to inhibit granulocyte adhesion and diapedesis. This study provides experimental evidence that SXNI may fulfill the need for stroke medicine targeting specifically at the recovery stage.

Abbreviations: SXNI, Shuxuening injection; G-CSF, granulocyte colony-stimulating factors; CIRI, cerebral ischemia-reperfusion injury; I/R, ischemia-reperfusion; MCAO, middle cerebral artery occlusion; mNSS, modified neurologic severity scores; IPA, ingenuity pathway analysis; RT-PCR, reverse transcription-polymerase chain reaction; ELISA, enzyme-linked immunosorbent assay; WB, western blot; IHC, immunohistochemistry; DEGs, differentially expressed genes; GBE, ginkgo biloba extract; TTLs, terpene trilactons; ECs, endothelial cells; TCM, traditional Chinese medicine; CCA, common carotid artery; ECA, external carotid artery; ICA, internal carotid artery; PPA, pterygopalatine; MCA, middle cerebral artery; TTC, 2, 3, 5-Triphenyl-2H-tetrazolium chlorid; H&E, hematoxylin & eosin; RNA-Seq, ribonucleic acid sequencing; BOS, base of support; RF, right front; RH, right hind; LF, left front; LH, left hind; FC, fold change; PPI, protein-protein interaction; UR, upstream regulators

* Corresponding author at: State Key Laboratory of Component-based Chinese Medicine, Tianjin University of Traditional Chinese Medicine, Beihua South Road, JingHai District, Tianjin, 301617, China.
E-mail address: yanzhu.harvard@icloud.com (Y. Zhu).
[1] Equal contribution to this work.

https://doi.org/10.1016/j.biopha.2020.110213
Received 4 February 2020; Received in revised form 19 April 2020; Accepted 28 April 2020

1. Introduction

Stroke is a brain disease with high mortality and disability [1,2], with ischemic stroke accounting for 87 % of all strokes [3]. Ischemic stroke is due to insufficient cerebral perfusion or blockage of blood vessels in the form of arterial embolism or thrombosis [4]. Currently, there are two main methods to treat ischemic stroke in clinic. One is intravenous thrombolysis by recombinant tissue-type plasminogen activator (tPA), but it has potential risk of hemorrhagic transformation [5,6] and with a narrow treatment window [7,8] that about 95 % of patients cannot receive treatment in time [9], resulting in residual neurological deficits [10]. Endovascular thrombectomy to restore cerebral blood flow is an alternative method for ischemic stroke patients [11,12]. However, the recovery of cerebral blood flow always causes reperfusion injury, exacerbates cerebral edema or hemorrhagic transformation [12–14] and increases the area of cerebral infarction [15], and gradually causes cognitive and motor dysfunction [16,17]. Thus, the development of more effective treatment for cerebral ischemia-reperfusion injury in stroke will help stroke patients with chronic disability [18].

Numerous animal experiments have shown that neuroprotective agents are effective against ischemic stroke, but failed in clinical transformation [19,20], which is largely related to the animal model designed [21]. Choosing the appropriate animal models is critical to transforming preclinical drugs into clinically useful anti-stroke drugs [22,23]. The intraluminal suture middle cerebral artery occlusion (MCAO) model is one of the most widely used animal models [21] and the closest to simulate human ischemic stroke [24,25]. In addition, clinical studies of stroke patients often use long-term (usually greater than 90 days) mortality and functional impairment as evaluation indicators, which better reflects the continued benefits of drugs in long-term survival [26]. However, our previous studies were limited to the protective effect on acute stroke mice (24 h), and ignored the longer-term treatment effects such as the subacute phase and the recovery phase [27,28]. Therefore, in this study, we set the experimental cycle to one week after stroke (subacute phase).

Ginkgo biloba extract (GBE) is a kind of product which is enriched with the active ingredients extracted from the leaves of Ginkgo biloba by using appropriate solvents. Its main pharmacological active ingredients include terpene trilactons (TTLs) and flavonols [29]. Ginkgolide A, ginkgolide B, ginkgolide C, ginkgolide J, and bilobalide are among the identified TTLs whereas kaempferol, quercetin, and isorhamnetin are among the identified flavonoids [30,31]. It is reported that Ginkgo biloba extract can treat neurodegenerative diseases [32], such as ischemic stroke [33,34], memory loss [35,36], epilepsy [37,38] and Alzheimer's disease [39–41]. It can also improve cognitive and neurological dysfunction after stroke [42,43]. Shuxuening Injection (SXNI) is a GBE approved by the Sino Food and Drug Administration [44]. We have previously shown that SXNI has a protective effect in mice with acute cerebral ischemia-reperfusion injury (CIRI) [27,28]. As mentioned in the previous paragraph, this time we administered SXNI to mice for 7 consecutive days to explore whether it could have a beneficial effect in the subacute phase of ischemic stroke. The use of minocycline has been shown to have a neuroprotective effect on ischemic stroke in stroke animals and clinical trials. Its mechanism of action may be related to anti-inflammatory [45–47], so we chose it as a positive drug.

Involvement of immune cells and inflammation in brain injury and recovery has been increasingly recognized as the frontier of neuroscience [48,49]. Granulocytes, a subgroup of leukocyte, are characterized by the presence of granules in their cytoplasm. There are four types of granulocytes, including neutrophils, basophils, eosinophils and mast cells [50]. The adhesion and diapedesis of granulocytes to endothelial cells (ECs) is an exceedingly essential pathway following brain injury, which is related to immunity/inflammation. It is reported to promote granulocyte, predominantly neutrophils, migration through the endothelium into the cerebral parenchyma, thereby causing neuroinflammation in cerebrovascular diseases such as stroke [51], atherosclerosis [52], and septic encephalopathy [53]. However, the classic cascade of leukocyte recruitment includes capture, rolling, adhesion, crawling, and transmigration, eventually crossing the blood-brain barrier into inflamed tissue [54,55]. Meanwhile, endothelial cells and immune cells produce a large number of granulocyte colony-stimulating factors (G-CSF/CSF-3) at the site of vascular injury [56–58], which are the main regulators of neutrophils [59–61]. Although G-CSF has been widely used in the treatment of chemotherapy-induced neutropenia [62], it has also been reported to aggravate the occurrence of various types of inflammation [63–66], which may be related to the induction of high expression of MAC-1 (CD11b/CD18) protein, E-selectin (CD62e) and its ligands, and to promote the migration of neutrophils to the site of inflammation [62,67–71]. Therefore, it is of scientific significance to study the role of G-CSF and granulocyte adhesion and inflammatory diapedesis in the treatment of stroke.

Consequently, the present study aimed to establish a subacute model of CIRI mimicking the immediate recovery phase of clinical stroke and investigate the therapeutic effect of SXNI on the neurological function of subacute stroke mice and its potential key mechanism. Our research shows that SXNI can exert neurotherapeutic effects on subacute stroke mice via inhibiting G-CSF-mediated the granulocyte adhesion and diapedesis pathway.

2. Materials and methods

2.1. Animals

A total of 110 male C57BL/6 J mice, weighing 22 − 25 g for 8 weeks, were purchased from Beijing Vital River Laboratory Animal Technology Co., Ltd. (Beijing, China, Certificate no.: SCXK Jing 2017 − 0005) and caged at a fixed humidity (40 % ± 5%) and temperature (22℃ ± 2℃), under 12 h light/12 h dark cycle, with free access to water and rat/mouse full nutrition jelly (J10001, Ready Biotechnology Co., Ltd, Shenzhen, China). This study was conducted in accordance with the recommendations by the Ministry of Science and Technology of China and the protocol for animal study was approved by the Laboratory Animal Ethics Committee of Tianjin University of TCM (Permit Number: TCM-LAEC2014004) and Tianjin International Joint Academy of Biotechnology and Medicine, China (Permit Number: JU20160024).

2.2. Establishment of cerebral ischemia-reperfusion (I/R) injury model and drug administration

After anesthetizing the mouse by inhalation with 2% isoflurane and placing them in a small animal respirator (RWD, Inc., China) filled with 1.5 % isoflurane, the left common carotid artery (CCA), left external carotid artery (ECA), left internal carotid artery (ICA) and left pterygopalatine (PPA) of the mouse were isolated for full exposure. Then, the CCA and ECA were tied with 6 − 0 medical suture respectively, and the distal end of ECA was burned by a monopolar electrical cautery later. The ICA was clamped with arterial hemostatic clip, and a small hole was cut in ECA to insert a silicone-coated 4 − 0 nylon monofilament (Jialing Biotechnology Co., Ltd., Guangzhou, China) to block the origin of the left middle cerebral artery (MCA), resulting in a decline of local cortical blood flow in the left MCA territory to approximately 20 % of the baseline. After 30 min the nylon monofilament was pulled out for blood flow reperfusion. In the sham group, only left CCA, ECA, ICA and PPA were separated and exposed, but no nylon monofilament was inserted. 110 mice were then randomly assigned to 6 groups (10 in sham group and 20 in other groups), including sham (saline), vehicle (I/R + saline), minocycline (I/R + minocycline, 15 mg/kg, M9190, Solarbio, Beijing, China, dissolved in saline and sterile-filtered through 0.22 μm) and the SXNI (drug approval number: Z13020795; batch number: 181108C1, Shineway Pharmaceutical Group Ltd, Hebei,

China) low (I/R + dose, 1.5 mL/kg), middle (I/R + dose, 3 mL/kg) and high (I/R + dose, 6 mL/kg). The drugs were administered from the tail vein immediately after I/R and every 12 h thereafter. The mice were killed by cervical dislocation and the brains were taken and rinsed in 0.9 % saline on the 7th day.

2.3. Evaluation of functional deficit

2.3.1. Neurological deficit score

As shown in previous researches [72,73], neurological deficit scores of mice were recorded on days 1, 4, and 7 after I/R based on the modified Neurological Severity Score (mNSS), including raising the mouse by the tail, walking on the floor, beam balance tests and reflexes absence. The score ranges from 0 to 14, and it was positively correlated with the severity of ischemia-reperfusion injury. Detailed scores can be found in the supplementary file Table S1.

2.3.2. Open-field test

On the 5th day after I/R, the mice were placed in an open field of 40 cm × 40 cm, with a high-speed camera hanging on the upper part. To eliminate odors, the bottom plate was wiped with 75 % alcohol before each animal was tested. Recording time was set to 30 min and the ANY-maze Behavioural Tracking Software (Stoelting Co. United States) was used to evaluate the parameters of total distance and average speed [74,75].

2.3.3. Locomotive gait analysis

As mentioned earlier [76,77], automatic quantitative gait analysis was implemented via using Catwalk system (Noldus Information Technology, Wageningen, Netherlands) on the 7th day after I/R. The top of the Catwalk system was covered with a ceiling with a light source. There are two black baffles in the middle to form a runway. The bottom of the system was a 1.5-meter glass floor with a high-speed camera under it. The mice were trained on the runway for two consecutive days before I/R to familiarize them with the runway. Utilizing Catwalk XT Version 9.1 software (Noldus Information Technology, Wageningen, Netherlands), the recovery of locomotive function after on the 7th day after I/R was evaluated by the base of support, max contact area, print area, swing speeds and stride length [78].

2.4. Measurement of cerebral infarction volume

The brain of the euthanized mouse was removed and rinsed in 0.9 % saline. 5 coronal sections were cut at 2 mm intervals in the brain mold, which were then transferred to 2 % 2, 3, 5-Triphenyl-2H-tetrazolium chloride solution (TTC, G3004, Solarbio, Beijing, China) solution and placed in a 37 ℃ incubator for 15 min [79]. The areas of the contralateral hemisphere (Ci), ipsilateral hemisphere (Ii), and ipsilateral non-ischemic region (Ni) were determined using the Image J software (National Institutes of Health, Bethesda, MD, United States), and the infarct volume (%) was calculated via the following formula [80]:

$$Infarct\ volume = \left(\frac{\Sigma i \left(\left(\frac{Ii - Ni}{Ii} \right) Ci \right)}{2 \Sigma i Ci} \right) * 100\%$$

2.5. Analysis of brain edema

After anesthetizing the mouse with 2 % isoflurane inhalation, the CT contrast agent (Iohexol Injection, 15 mL/kg, H20000595, General Electric Pharmaceutical Co., Ltd. Shanghai, China) was injected via the tail vein. Then used the μCT small animal imager (Quantum FX; PerkinElmer, United States) to perform a 360-degree scan of the brain under the following parameters: voltage 90 kV, current 180 μA, field of vision 20 mm, scanning technology 4.5 min. Finally, the offset distance of the midline was quantified via utilizing ImageJ software (National Institutes of Health, Bethesda, MD, United States) [81]. The longer the offset distance, the more severe the brain edema.

2.6. Hematoxylin and eosin staining (H&E)

As previously described [28], brain tissue of mice was fixed in 4% paraformaldehyde solution for at least 48 h. The brain slices were dehydrated in an automatic dehydrator (Excelsior, Thermo., Ltd., United States) for about 16 h, and then removed and embedded in paraffin. The paraffin blocks were manually cut (Gemini, Thermo., Ltd., United States) into 5 μm sheets, which were attached to a glass slide and dried, and followed stained via using automatic staining machine (ClearVue, Thermo., Ltd., United States). The slides were sealed by an automatic sealing machine (ClearVue, Thermo, Ltd., USA), which were later photographed with an optical microscope (Vectra 3, PerkinElmer, United States) and pathologically analyzed.

2.7. Ribonucleic acid sequencing (RNA-Seq) and data analysis

Total RNA was extracted from brain tissue and tested for purity and integrity. The library of transcriptome sequencing was then generated using NEBNext® UltraTM RNA Library Prep Kit for Illumina® (NEB, USA), and the library quality was detected with Qubit2.0 Fluorometer and Agilent 2100 bioanalyzer. In addition, the library preparations were sequenced on an Illumina Novaseq platform. After obtaining clean data (clean reads) by deleting the reads containing adapter, reads containing ploy-N, and low-quality reads in the original data, these clean reads were compared to the *Mus musculus* genome utilizing the HISAT2 alignment software (The Johns Hopkins University, Baltimore, Maryland, United States). The quantification of gene expression level was then quantified using FPKM. Differential expression analysis of mice from the vehicle and SXNI middle groups was performed utilizing the DESeq2 R package (1.16.1). log2FoldChange ≥ 1.5 and P-value ≤ 0.01 were set as the threshold of significant difference expression.

2.8. Core analysis of differentially expressed genes (DEGs)

The core analysis of DEGs obtained by RNA-Seq was carried out by Ingenuity® Pathway Analysis (IPA). The DEGs with fold change ≥ 1.5, P-value ≤ 0.01 and fold change ≥ 10, P-value ≤ 0.01 were entered into Ingenuity's Knowledge Base and then core analysis was performed respectively. In addition, the following settings were made during data analysis: Ingenuity Knowledge Base was used as a reference set; endogenous chemicals were not included; direct and indirect relationships. Significance was measured by the number of molecules mapped to the pathway dataset divided by the total number of genes in the pathway and P-value of Fisher's exact test.

2.9. RNA extraction and RT-PCR assay

According to the manufacturer's protocols, total RNA samples were extracted from the affected side of brain tissue with EasyPure® RNA Kit (ER101, TransGen Biotech, Beijing, China), and then transcribed into cDNA with the Transcriptor First Strand cDNA Synthesis Kit (04897030001, Roche, Mannheim, Germany). The cDNA was mixed with Bestar™ qPCR MasterMix (2043, DBI Bioscience, Shanghai, China) and primers in PCR® Strip Tubes (Corning, New York, USA), and they were transferred to real-time PCR system (LightCycler®480, Roche, Germany). The mRNA expression levels of each sample were detected. The primers used in this experiment include *G-csf, Tnf, Il1b, Il6, Ccl2, Ccr2, Cxcr2, Cxcl2, Cxcl10, Sele, Selp, Esl-1, Psgl-1, Itgam (Mac-1), Itgal (Lfa-1), Icam-1*and *Icam-2*. Their relative mRNA levels were determined using glyceraldehyde-3-phosphate dehydrogenase (*Gapdh*) as a standard. All the above primers were synthesized by Sangon Biotech (Shanghai, China) and shown in Table 1.

Table 1
Primer sequences.

Gene	Forward Primer (5′–3′)	Reverse Primer (5′–3′)
G-csf	ATGGCTCAACTTTCTGCCCAG	CTGACAGTGACCAGGGGAAC
Tnf	CCCTCACACTCAGATCATCTTCT	GCTACGACGTGGGCTACAG
Il1b	GCAACTGTTCCTGAACTCAACT	ATCTTTTGGGGTCCGTCAACT
Il6	TAGTCCTTCCTACCCCAATTTCC	TTGGTCCTTAGCCACTCCTTC
Ccl2	TTAAAAACCTGGATCGGAACCAA	GCATTAGCTTCAGATTTACGGGT
Ccr2	ATCCACGGCATACTATCAACATC	CAAGGCTCACCATCATCGTAG
Cxcr2	ATGCCCTCTATTCTGCCAGAT	GTGCTCCGGTTGTATAAGATGAC
Cxcl2	CCAACCACCAGGCTACAGG	GCGTCACACTCAAGCTCTG
Cxcl10	CCAAGTGCTGCCGTCATTTTC	GGCTCGCAGGGATGATTTCAA
Sele	ATGCCTCGCGCTTTCTCTC	GTAGTCCCGCTGACAGTATGC
Selp	CATCTGGTTCAGTGCTTTGATCT	ACCCGTGAGTTATTCCATGAGT
Psgl-1	GTCTGTCCCGTCACTGGATAC	TTCTCTCTTACCGGGTTACCA
Esl-1	CAAGATGACGGCCATCATTTTCA	TTCCCCAAGACGAATGCTGC
Mac-1	ATGGACGCTGATGGCAATACC	TCCCCATTCACGTCTCCCA
Lfa-1	CCAGACTTTTGCTACTGGGAC	GCTTGTTCGGCAGTGATAGAG
Icam-1	GTGATGCTCAGGTATCCATCCA	CACAGTTCTCAAAGCACAGCG
Icam-2	TGGTCCGAGAAGCAGATAGTAG	GAGGCTGGTACACCCTGATG
Gapdh	TGGTGAAGCAGGCATCTGAG	TGCTGTTGAAGTCGCAGGAG

2.10. Enzyme-linked immunosorbent assay (ELISA)

On the 7th day after I/R, the plasma of mice was collected, and its upper serum was separated by centrifugation at 1000 r/min for 15 min. According to the protocol of the manufacturer of Mouse G-CSF ELISA Kit (SEKM-0040, Solarbio, Beijing, China), the OD value of each sample at a wavelength of 450 nm was measured by Tecan SPARK microplate reader (Tecan, Groedig, Austria). The OD value was substituted into the standard curve to obtain the G-CSF protein concentration in the serum.

2.11. Western blotting (WB)

The brain tissue was treated with RIPA buffer (Solarbio, Beijing, China), and the supernatant was centrifuged at 13,000 r/ min and 4°C for 10 min. Then the total protein concentration of the supernatant was measured with BCA Protein Assay Kit (PC0020, TransGen Biotech, Beijing, China). The SDS-PAGE protein loading buffer (P0015 L, Beyotime Biotechnology, Shanghai, China) was added to the supernatant, and the protein was deformed by heating in a metal bath at 95°C for 10 min. The protein samples were separated by SDS-polyacrylamide gel electrophoresis and transferred to the PVDF membrane. The total protein on PVDF membrane was sealed with 5% skimmed milk. The primary antibody (Rabbit anti-E-Selectin, 1:2000, bs-1273R, Bioss Inc., Beijing, China and GAPDH, 1:4000, 14C10, Cell Signaling Technology, Beverly, MA) was added dropwise to the PVDF membrane and transferred to a 4 ˚C refrigerator for 8 h. After washing it with TBS-T, the secondary antibody (Goat anti-Rabbit lgG, 1:4000, ZB-2301, ZSbio, Beijing, China) was added dropwise to the PVDF membrane and incubated at room temperature for 2 h, and then washed with TBS-T again. Finally, the EasySee Western Blot Kit (DW101-02, TransGen Biotech, Beijing, China) was used to react with the PVDF membrane for 1 min under darkness, and the bands were obtained by the gel imaging system. The protein expression of E-selectin was analyzed via using ImageJ analysis software (National Institutes of Health, Bethesda, MD, USA) and standardized to GAPDH.

2.12. Immunohistochemistry (IHC)

The paraffin sections of brain tissue were baked in an oven at 60°C for 1 h to melt the paraffin, then dewaxed in xylene and rehydrated. After inhibiting endogenous peroxidase activity with 3% H_2O_2, the tissue sections were heated in 0.01 M sodium citrate buffer (pH 6.0) and allowed to cool to normal temperature. Non-specific binding sites were blocked with blocking buffer (10 % bovine serum) for 1 h at 37 ˚C. The sections were incubated with Rabbit Anti-MAC-1(CD11b/CD18) antibody (bs-1014R, Bioss Inc., Beijing, China) diluted in blocking buffer (1: 300) for 2 h at 37 ˚C and washed twice with PBS-T (0.01 M PBS pH 7.4: KH_2PO_4 0.02 %, N_2HPO_4 0.29 %, KCl 0.02 %, 0.8 % NaCl, 0.05 % BSA, Tween-20 0.05 %, 0.0015) for 5 min each. Then, the biotin-conjugated goat anti-rabbit IgG (ZB-2010, ZSbio, Beijing, China) diluted in blocking buffer (1: 200) was added dropwise and incubated at 37 ˚C for 40 min, and the sections were washed in PBS-T twice, for 5 min each time again. DAB kit (AR1022, Boster Bio., Wuhan, China) was used for color development, followed by counter staining with hematoxylin and differentiation with 1% hydrochloric acid alcohol. Finally, seal the sections with neutral gum after dehydration. The expression of MAC-1 was detected by optical microscope (Vectra 3, PerkinElmer, United States) and quantified by calculating its integrated optical density value and positive cells using ImagePro Plus software (National Institutes of Health, Bethesda, MD, United States).

A graphical abstract of all the above experiments can be found in the supplementary file Fig. S1.

2.13. Statistical analysis

All data was expressed as mean ± SEM or mean ± SD. Statistical analysis was carried out using Student's two-tailed *t*-test for comparison between two groups and One-way analysis of variance (ANOVA) for three or more groups by SPSS 22.0. Value of $P < 0.05$ was considered statistically significant.

3. Results

3.1. Effects of SXNI on survival rate, neurological deficit and exercise ability in subacute stroke mice

High mortality was one of the main characteristics of ischemic stroke. By recording the survival of the mice within 7 days after ischemia-reperfusion, we found that compared with the sham group, the mice in vehicle group had a higher mortality rate. However, the treatment with minocycline and 3 doses of SXNI reduced mortality compared to the vehicle group (Fig. 1A). mNSS was an important indicator to evaluate the severity of neurological damage after stroke. The mNSS score of mice on the 1 st, 4th and 7th day after stroke showed there were obvious neurological disorders in vehicle group and each administration group compared with sham group on the 1 st day, but on the 4th and 7th day, minocycline, middle doses of SXNI (3 mL/kg) and high doses of SXNI (6 mL/kg) could significantly reduce neurological deficit scores of subacute stroke mice compared with vehicle group (Fig. 1B). In addition, the open field test on the 5th day after stroke found that exercise speed and distance of the vehicle group mice were remarkedly declined compared with those in sham group (Fig. 1C, D). However, compared with the vehicle group, the exercise speed and distance of mice were significantly increased in the minocycline, SXNI middle (3 mL/kg) and SXNI high (6 mL/kg) groups (Fig. 1C, D).

3.2. Effect of SXNI on locomotive gait in subacute stroke mice

Another pathological feature after stroke was gait dysfunction, especially on the contralateral limb. The catwalk parameters were shown in Fig. 2A. The middle doses SXNI (3 mL/kg) could significantly improve the decrease of base of support (BOS) in the front paws and hind paws caused by I/R. Compared with sham group, the max contact area, print area, stride length and swing speed of the right front, right hind and left hind of vehicle group mice were obviously reduced, while minocycline and the middle doses SXNI (3 mL/kg) could remarkedly ameliorate the max contact area, print area and stride length compared with vehicle group (Fig. 2C–F). In addition, the high doses SXNI (6 mL/kg) also significantly increased max contact area and stride length in the right hind and left hind of subacute stroke mice, while the low doses SXNI (1.5 mL/kg) only increased stride length in the left hind compared

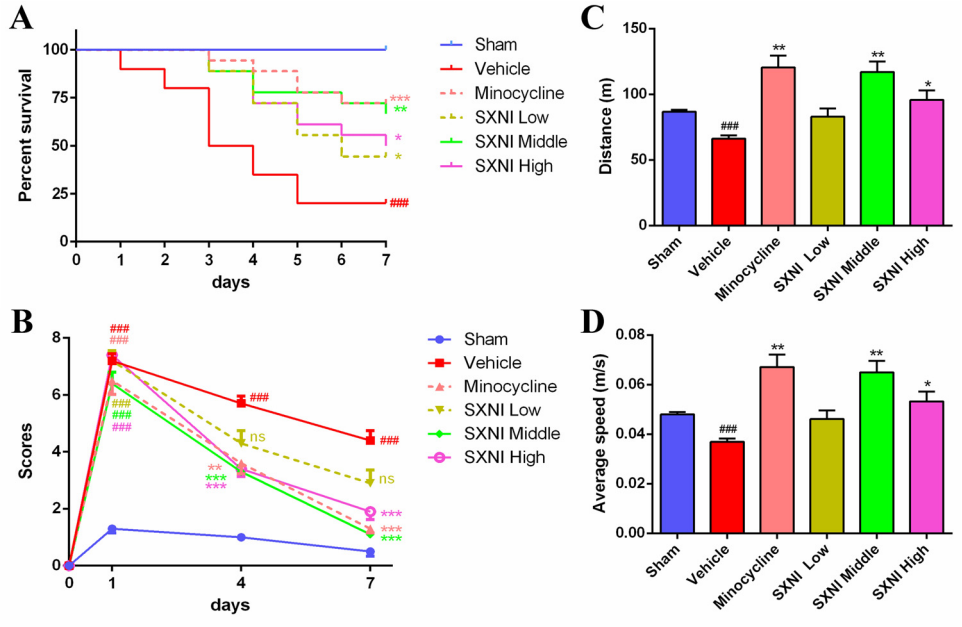

Fig. 1. SXNI improved survival rate, neurological deficit score and locomotor function in subacute stroke mice. Within 7 days after stroke, the survival of each group of mice was recorded, and neurological and motor function tests were performed. (A) Survival curve of mice in each group within 7 days after stroke (n = 10 ~ 20). (B) Modified neurologic severity scores on post-stroke day 1, 4 and 7 (n = 10). The locomotor function of each group of mice was evaluated on the 5th day after the stroke. (C) The motor distance and (D) average speed of mice were calculated via using open field locomotion chambers (n = 8). Data were expressed as mean ± SEM. $^{###}P < 0.001$ vs. Sham group, $^{*}P < 0.05$, $^{**}P < 0.01$ $^{***}P < 0.001$ vs. Vehicle group.

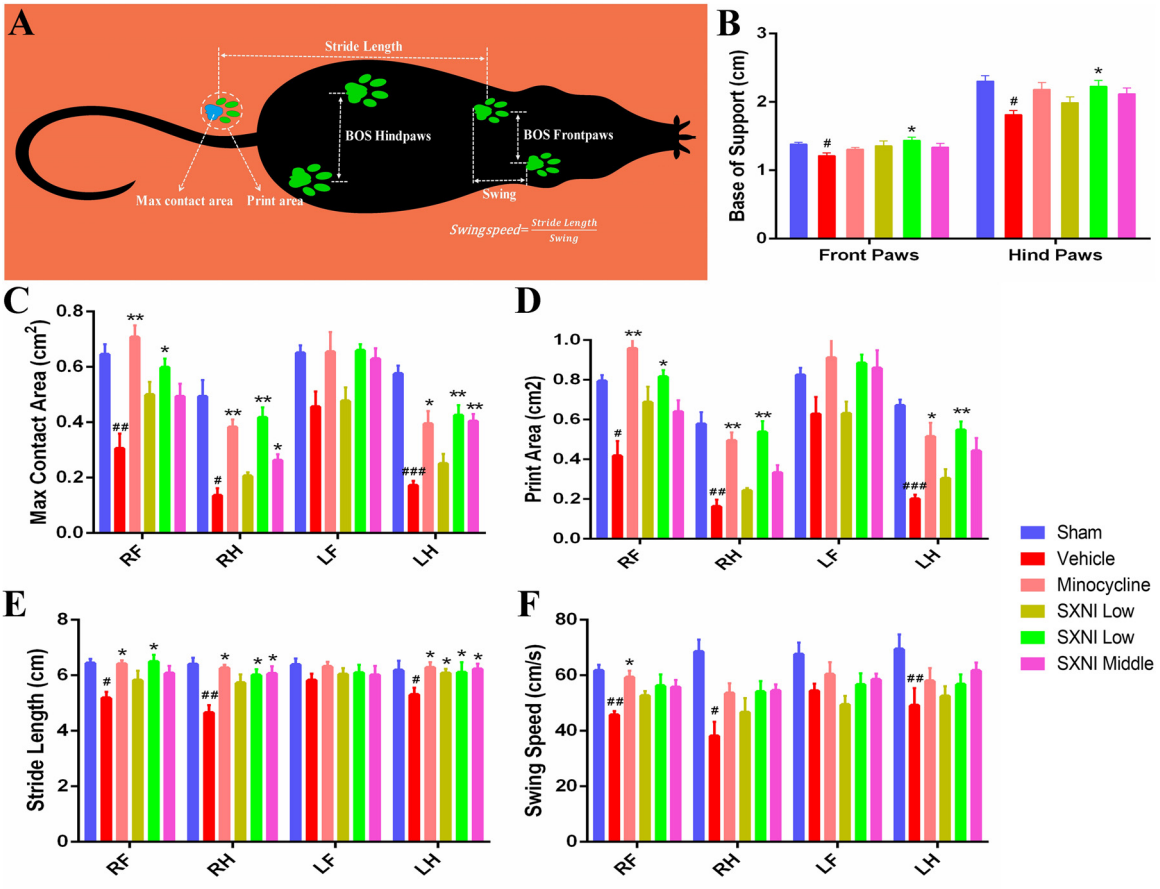

Fig. 2. SXNI ameliorated motor gait in subacute stroke mice. 7 days after stroke, the locomotive gait of the mice was tested using the Catwalk system. (A) Graphical representation of selected gait parameters. (B) Quantification of BOS in front and hind paws, and quantification of (C) maximum contact area, (D) print area, (E) stride length and (F) swing speed of four paws in mice (n = 6). RF: right front; RH: right hind; LF: left front; LH: left hind. Data were expressed as mean ± SEM. $^{#}P < 0.05$, $^{##}P < 0.01$, $^{###}P < 0.001$ vs. Sham group, $^{*}P < 0.05$, $^{**}P < 0.01$ vs. Vehicle group.

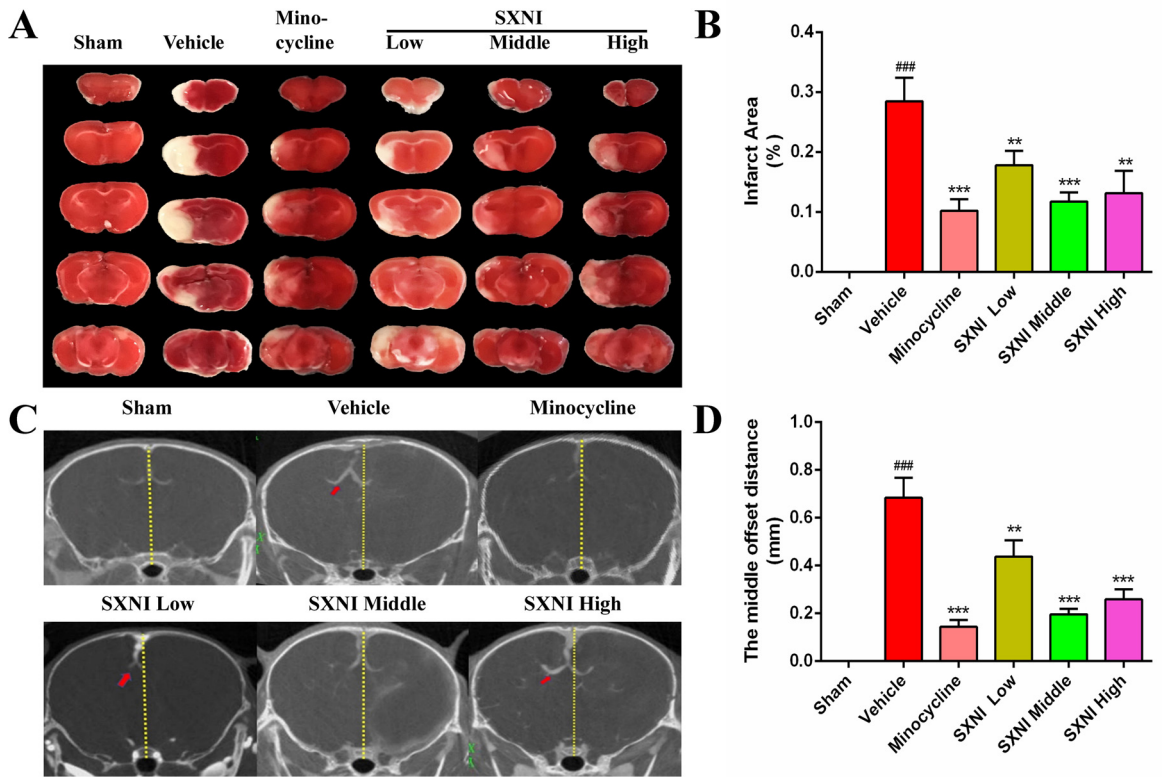

Fig. 3. SXNI reduced cerebral infarct size, brain edema in subacute stroke mice. On post-stroke day 7, the brain tissue of mice was stained with TTC and H&E, and imaged by micro-CT. (A) Representative images of TTC staining in different groups. White area indicates ischemic infarction area. (B) Quantification of infarct volume after different treatment (n = 6 in each group). (C) Representative micro-CT images in each group. Brain midline offset distance positively correlated with the severity of cerebral edema. (D) Quantitation of the offset distance of midline after different treatment (n = 6 in each group). Data were expressed as mean ± SD. $^{###}$P < 0.001 vs. Sham group, *P < 0.05, **P < 0.01, ***P < 0.001 vs. Vehicle group.

with vehicle group.

3.3. The effects of SXNI on brain damage in subacute stroke mice

By quantifying the infarct volume in TTC-stained brain sections and indirectly calculating the severity of brain edema in micro-CT imaging, the severity of brain injury in mice on the 7th day after stroke was estimated. Compared with the sham group, the cerebral infarction area (Fig. 3A, B) and middle offset distance (Fig. 3C, D) were significantly increased in the vehicle group mice. SXNI and minocycline treatment obviously reduced the area of cerebral infarction (Fig. 3A, B) and the degree of edema (Fig. 3C, D) compared with the vehicle group. Simultaneously, the histopathological examination of brain tissue from the vehicle group revealed extensive structural abnormalities, including increased necrosis, fusion areas, and infiltration of inflammatory cells, which were indicated by yellow arrows (Fig. 4). In contrast, after administration with SXNI and minocycline, the damaged histological features and brain structure were remarkedly improved (Fig. 4). Therefore, SXNI could significantly improve the brain damage of mice after stroke via reducing the area of cerebral infarction, cerebral edema and pathological changes of brain tissue.

3.4. Transcriptome identification of DEGs between vehicle group and SXNI group

In order to identify SXNI gene targets in brain tissue, high-throughput sequencing analysis was performed on the brain tissue of I/R mice with or without SXNI (3 mL/kg) treatment. Transcriptome results showed that there were 28,258 expressed genes in the SXNI treatment group mice and 27,463 expressed genes in the vehicle group mice. In total, 963 DEGs with Fold-Change values greater than or equal to 1.5 and P-values less than or equal to 0.01 were selected, including 495 up-regulated genes and 468 down-regulated genes (Fig. 5A). Their detailed information was listed in Supplementary Table S2. In addition, Fig. 5B showed the overall gene expression profile of a hierarchical cluster of the above 963 DEGs.

3.5. Key pathways and targets of SXNI in the treatment of subacute stroke mice

The core analysis of DEGs obtained by high-throughput sequencing analysis was carried out via using IPA. In order to increase the accuracy of the analysis results, the thresholds of DEGs were set to FC ≥ 1.5, P ≤ 0.01 and FC ≥ 10, P ≤ 0.01 respectively, and the selected DEGs were imported into Ingenuity's Knowledge Base to determine the primary pathway regulated by SXNI. The classic pathways were ranked based on the -log (p-value) score, and the top 20 was listed (Fig. 6A). Notably, granulocyte adhesion and diapedesis pathway ranked first in the above two rankings (Fig. 6A). Therefore, it was regarded as the most critical pathway regulated by SXNI in the treatment of subacute-stroke mice. However, DEGs with FC ≥ 1.5 and P ≤ 0.01 were analyzed in further core analysis. According to the -log(p-value) score, the top 5 biological functions are displayed in a decending order: immune response, inflammation, angiogenesis, vasculogenesis and apoptosis (Fig. 6B, C). Meanwhile, the protein-protein interaction (PPI) and upstream regulators (UR) analysis results of DEGs with FC ≥ 1.5 and P ≤ 0.01 indicate that there are 26 overlapping genes (Fig. 6D–F). Through literature review, 13 genes related to stroke, including *G-csf*, *Ngp*, *S100a9*, *Cxcl2*, *Saa1*, *S100a8*, *Lcn2*, *Il6*, *Cxcr2*, *Nos2*, *Mmp8* and *Ccl2*, were selected as potential major targets of SXNI (Fig. 6G). Among them, the fold change of *G-csf* was down by 1957-fold, which was an striking change. In summary, the most critical pathway and target of SXNI by

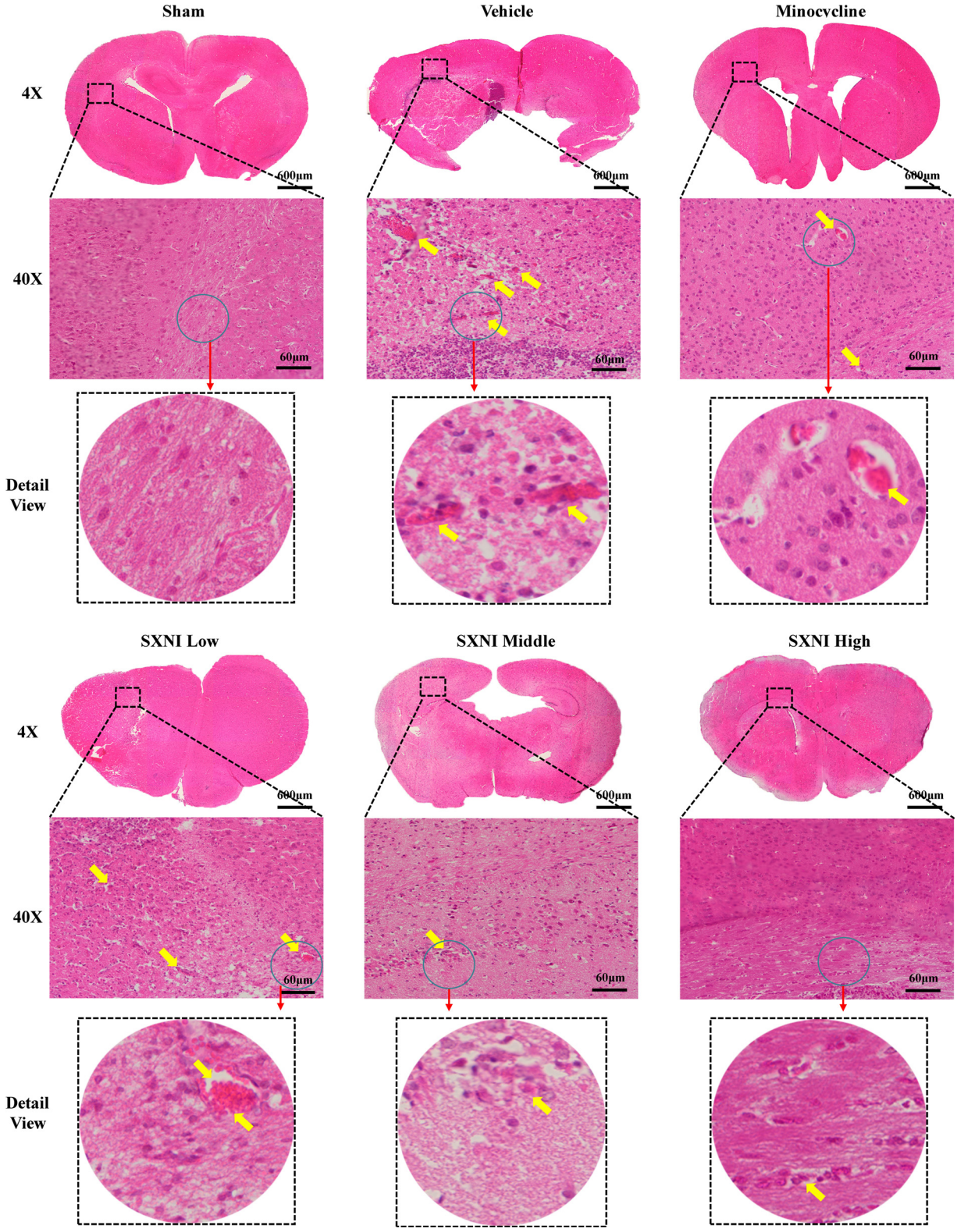

Fig. 4. SXNI reduced histopathological changes in subacute stroke mice. On post-stroke day 7, the brain tissue of mice was stained with H&E. Representative images of histopathological changes, including structural disorders and inflammatory cell infiltration indicated by yellow arrows. (4×, 40× magnification and detail view, n = 4 in each group).

transcriptome analysis appear to be granulocyte adhesion and diapedesis pathway and G-CSF, respectively, which are validated experimentally next.

3.6. Verification of important DEGs at the mRNA level in the granulocyte adhesion and diapedesis pathway

It was found from Fig. 6F that most of the important DEGs were cytokines, such as *G-csf*, *Tnf*, interleukins (including *Il1a*, *Il1b*, *Il6*),

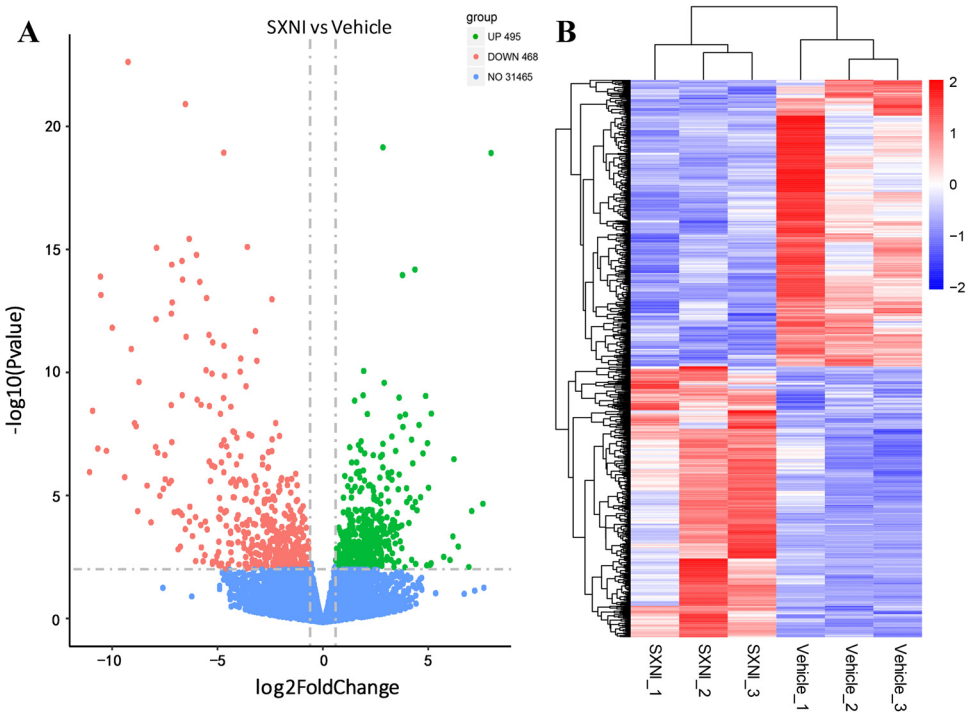

Fig. 5. Differentially expressed genes (DEGs) of SXNI group and vehicle group mice. The distribution of DEGs (fold change ≥ 1.5 and p-Value ≤ 0.01) was visually presented by the volcanic map. (A) Distribution of DEGs between SXNI (3 mL/kg) and the vehicle group mice. The abscissa represents the fold change in the two groups, and the ordinate represents the significance level of gene expression between the two groups. Red dots indicate up-regulated genes, while green dots indicate down-regulated genes (n = 3). (B) Hierarchical cluster analysis between samples from the SXNI (3 mL/kg) group and the vehicle group.

chemokine (including *Ccl2*, *Ccr2*, *Cxcr2*, *Cxcl2* and *Cxcl10*), among which the fold change of *G-csf* was the largest in transcriptome analysis. RT-PCR was used to verify the accuracy of the transcriptome results. The results of RT-PCR were consistent with those of transcriptome, that is, SXNI can significantly down-regulate *G-csf*, *Tnf*, *Il1b*, *Il6*, *Ccl2*, *Ccr2*,*Cxcr2*, *Cxcl2* and *Cxcl10* (Fig. 7B), which proved that the transcriptome data had high reliability and biological repeatability. Besides, RT-PCR results of genes closely related to the granulocyte and diapedesis pathway showed that the expression levels of *Sele* (*E-selectin*), *Selp* (*P-selectin*), *Mac-1*, *Laf-1*, *Esl-1*, *Psgl-1*, *Icam-1* and *Icam-2* were also significantly decreased after SXNI administration compared with the vehicle group mice (Fig. 7C).

3.7. Effect of SXNI on the expression levels of G-CSF, E-selectin and MAC-1 proteins in subacute stroke mice

Significant targets in the granulocyte adhesion and diapedesis pathway were verified at the protein level. The ELISA experiment showed that compared with the sham group, the G-CSF protein level in serum was remarkedly increased in the mice of vehicle group. The middle (3 mL/kg) and high (6 mL/kg) doses of SXNI were able to obviously down-regulate the abnormally elevated G-CSF after stroke (Fig. 8A). WB experiments indicated E-selectin was significantly increased in the brain tissue of mice in the vehicle group, while different doses of SXNI could substantially reduce the expression of E-selectin (Fig. 8B, C). In addition, IHC experiments demonstrated that SXNI can reverse the abnormal elevation of MAC-1 protein in brain tissue caused by stroke (Fig. 8D–F). Interestingly, treatment with minocycline did not play a role in the expression of G-CSF, E-selectin, and MAC-1 in comparison to vehicle (Fig. 8A, C, E, F), suggesting that minocycline may not play a role in neurofunctional recovery via down-regulating the expression of these proteins or inhibiting granulocyte adhesion and diapedesis pathway.

4. Discussion

Despite of intensive efforts worldwide, the development of medicine for post-stroke recovery has been disappointing. The failure of stroke recovery drugs in clinical translation is related to many factors, including dose response, therapeutic window, outcome measures, physiological monitoring, multiple species [23]. Unlike acute stroke, restoring post-stroke behavioral activity dependents in part on neurological recovery [82]. Therefore, selecting appropriate animal stroke models and behavioral evaluation indicators can better simulate the occurrence and development of human stroke, and align preclinical to clinical stroke recovery studies, thereby maximizing the efficiency of clinical translation of anti-stroke drugs [83]. Our current study attempts to fillin this need by creating a mouse model mimicing the clinical subacute phase of stroke by milder ischemia and extended reperfusion. With this model, we were able to better evaluate the behavial deficiency and improvement after drug treatment, as well as to better examine the molecular events distinguishing those occurring at the acute phase of stroke.

In previous studies, we have shown that SXNI plays a protective role in acute CIRI mice through the atherosclerosis signal and inflammatory response mediated by Tnfrsf12a [27]. Besides, the main components of SXNI, ginkgo flavonol glycosides or ginkgolides act differently in cerebral vs myocardial I/R injury. In particular, the latter preferentially reduces CIRI via regulation of TWEAK-Fn14 signaling pathway [28]. However, these studies were carried out during the acute ischemic stroke, which was difficult to reflect the beneficial role of SXNI in the longer recovery period. Using the newly established post-stroke recovery model in this study that extended the administration time to 7 days after stroke, we are able to investigate whether SXNI can play a role in facilitating neurofunctional recovery in subacute stroke, so as to find anti-stroke drugs that can be used clinically.

Since it was well known that stroke has the characteristics of eating difficulties [84,85] and high mortality [86], we recorded the changes in body weight and survival of mice within 7 days after stroke, and found that the middle doses of SXNI (3 mL/kg) can significantly improved weight changes (Fig. S2) and survival (Fig. 1A) of mice after stroke. In addition, since stroke often lead to hemiplegia, limb flexion, and motor dysfunction, we used different behavioral evaluation methods, including mNSS [73,87], open-field test [88,89], and Catwalk [90,91], to assess neuromotor function of subacute stroke mice. Significantly, both mNSS and open-field test results indicated that SXNI at 3 mL/kg and 6

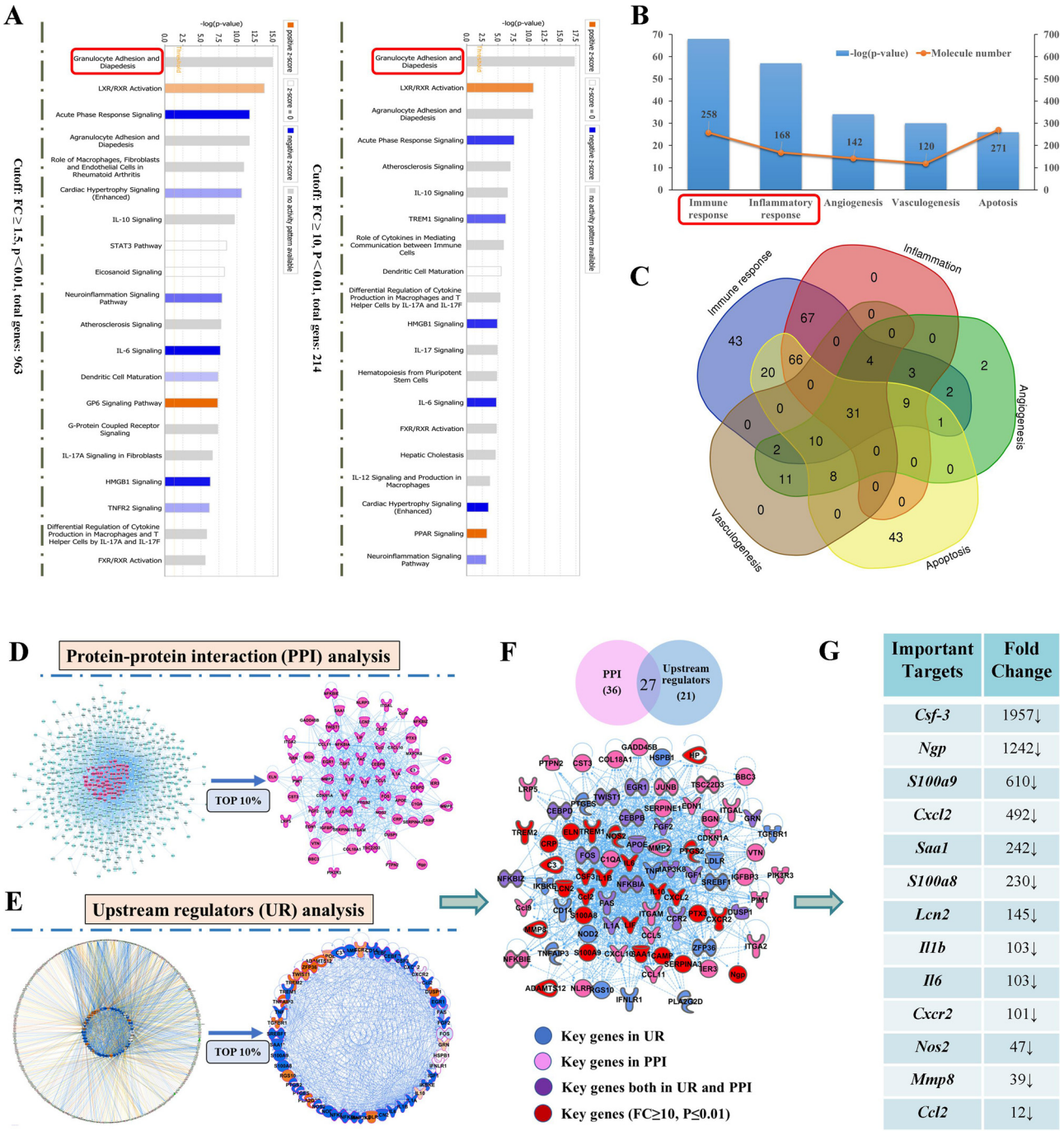

Important Targets	Fold Change
Csf-3	1957↓
Ngp	1242↓
S100a9	610↓
Cxcl2	492↓
Saa1	242↓
S100a8	230↓
Lcn2	145↓
Il1b	103↓
Il6	103↓
Cxcr2	101↓
Nos2	47↓
Mmp8	39↓
Ccl2	12↓

Fig. 6. SXNI-regulated critical pathways and targets in subacute stroke mice. (A) There were 963 DEGs with FC ≥ 1.5 and p < 0.01, and 214 DEGs with FC ≥ 10 and P < 0.01. Core analysis revealed the top 20 pathways of the above DEGs. According to the -log(p-value) score, the granulocyte adhesion and diapedesis pathway was number one in both rankings. (B) The top 5 biological functions were displayed based on -log (p-value), and (C) a Venn Diagram. (D) The PPI analysis revealed 63 important DEGs, (E) while the UR analysis pointed out 48 important DEGs. (F) Key genes in both PPI and UR and key genes with FC ≥ 1.5 and P ≤ 0.01. (G) 13 important targets that may be related to stroke and their fold changes (3 mL/kg of SXNI vs Vehicle).

mL/kg can obviously ameliorate the neurological function and motor capacity of subacute stroke mice (Fig. 1B–D). Gait analysis showed that SXNI can reverse limb dyskinesia caused by stroke to varying degrees, including BOS, maximum contact area, print area, stride length and swing speed, among which the hind limb and the contralateral limb of mice were more affected, which was consistent with the results of other studies [92]. On the 7th day after stroke, TTC staining results of the brain tissue of mice displayed that all three doses of SXNI can reverse their brain damage, and traces of recovery can be clearly seen (Fig. 3A, B). The results was consistent with that of Micro-CT (Fig. 3C, D), that SXNI can remarkedly reduce cerebral infarction and cerebral edema volume in subacute stroke mice. H & E staining of pathological sections showed that SXNI could significantly improve the structural disorder and inflammatory cell infiltration of brain tissue caused by stroke (Fig. 4).

We selected the effective dose of SXNI (3 mL/kg) for RNA-Seq, aiming to explore the main ways in which SXNI can help subacute stroke recovery. The DEGs of stroke mice in the vehicle group and SXNI group (3 mL/kg) was obtained by RNA-Seq, and DEGs with fold change ≥1.5 and p values ≤ 0.01 (Supplementary Table S2) were analyzed by

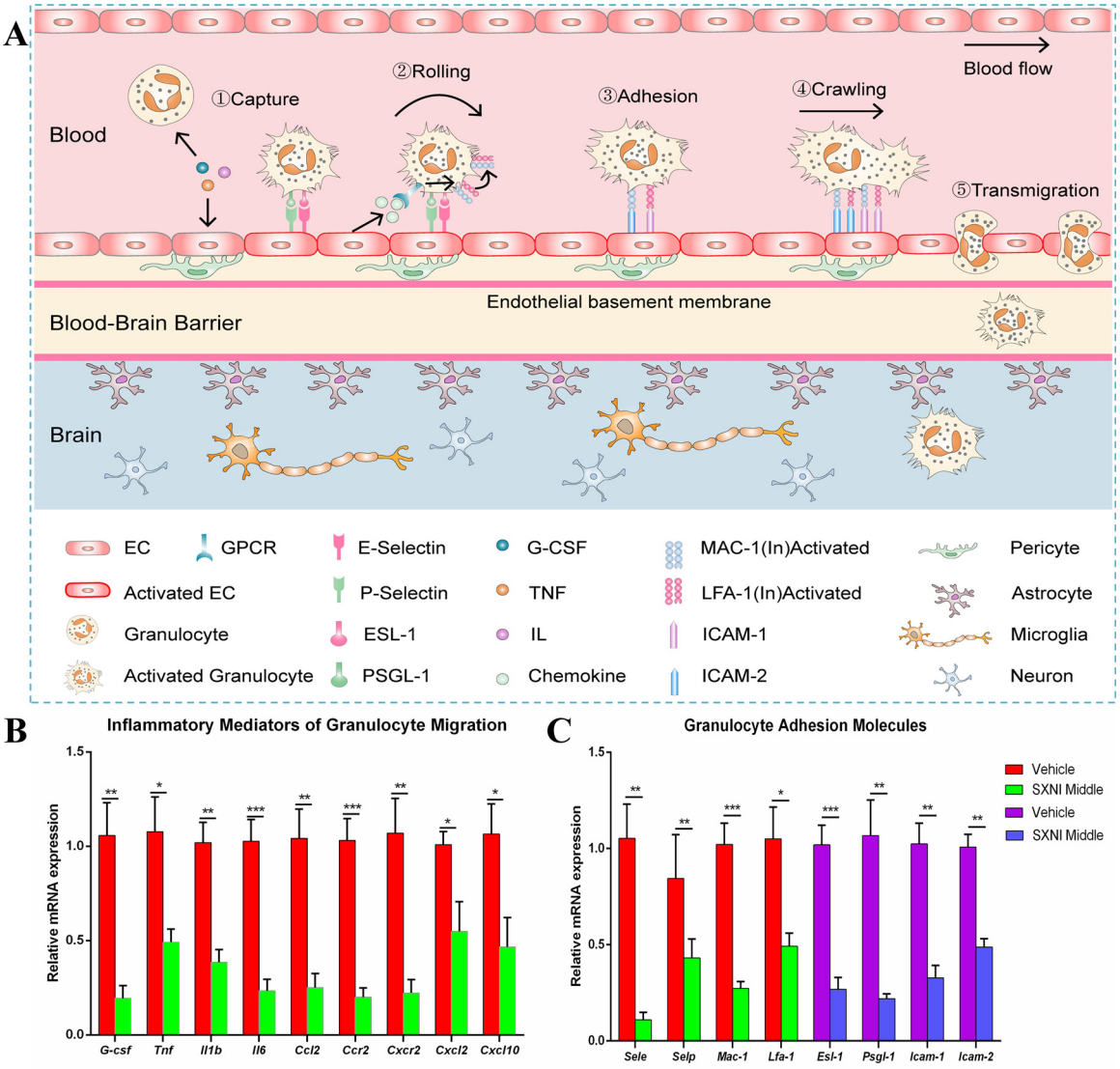

Fig. 7. Validation of genes regulated by SXNI related to granulocyte adhesion and diapedesis. (A) Schematic diagram of the granulocyte adhesion and diapedesis pathway involved in immune/inflammatory response in brain after stroke, including related pro-inflammatory factor-mediated capture, rolling, adhesion, crawling and transmigration. (B) The immune/inflammatory mediators with obvious changes in both transcriptome and IPA analysis were verified by RT-PCR, including *G-csf, Tnf, Il1b, Il6, Ccl2, Ccr2, Cxcr2, Cxcl2 and Cxcl10* (n = 5). (C) RT-PCR experiments were also performed to detect the mRNA expression of granulocyte adhesion molecules, including *Sele, Selp, Mac-1, Lfa-1, Psgl-1, Esl-1*, *Icam-1* and *Icam-2,* with red and green DEGs from transcriptome (n = 5). Data were expressed as mean ± SEM. *P < 0.05, **P < 0.01, ***P < 0.001 vs. Vehicle group.

IPA. As can be seen from Fig. 6A and B, the most relevant pathway was granulocyte adhesion and diapedesis and the most relevant functions were immune response and inflammatory response As we all know, the granulocyte adhesion and diapedesis pathway plays an important role in immune and inflammatory responses [93,94], which are mainly related to inflammatory mediators and cell adhesion molecules [94,95]. In order to verify the accuracy of the analysis results, we selected 9 representative mediators of granulocyte migration such as *G-csf*, *Tnf*, *Il1b*, *116*, *Ccl2*, *Ccr2*, *Cxcr2*, *Cxcl2* and *Cxcl10*, and 8 important granulocyte adhesion molecules such as *Sele*, *Selp*, *Esl-1*, *Psgl-1*, *Mac-1*, *Lfa-1*, *Icam-1* and *Icam-2* for RT-PCR verification. The verification results were consistent with the RNA-Seq results, which showed that the RNA-Seq results have higher accuracy and repeatability.

Under normal circumstances, granulocytes circulate in the blood along the direction of blood flow. When receiving inflammatory signals such as G-CSF, TNF, IL1, IL6 caused by stroke, granulocytes will adhere to ECs and eventually infiltrate the brain, aggravating the development of inflammation. Specifically, on the one hand, inflammatory mediators (such as G-CSF, TNF, IL1) activate ECs to secrete E-selectin and P-selectin [96,97]. The E-selectin and P-selectin bind to their respective ligands, PSGL1 and ESL1, on the granulocytes, resulting in capture and rolling [98,99]. On the other hand, activated ECs release chemokines through transcytosis [100–102], and chemokines interact with GPCRs to activate MAC-1 and LFA-1 on granulocytes [103,104]. Both MAC-1 and LFA-1 can interact with ICAM-1 and ICAM-2 on ECs [105–107], allowing granulocytes to adhere to ECs and crawl along the direction of blood flow until paracellular or transcellular transmigration [108]. Eventually cross the blood-brain barrier to the cerebral infarcted area (Fig. 7A). Some studies had reported that overexpression of endogenous G-CSF may exacerbate the occurrence and development of inflammation in stroke mice, which may be achieved by stimulating the secretion of water-soluble E-selectin and MAC-1 [109,110]. Therefore, we measured G-CSF in mouse serum and E-selectin and MAC-1 in brain tissue on the 7th day after stroke. The results indicated that G-CSF, E-selectin and MAC-1 were significantly expressed in mice after stroke, while SXNI could inhibit their expression (Fig. 8). Remarkedly, the SXNI-induced change of *G-csf* in the granulocyte adhesion and diapedesis pathway by RNA-Seq reached more than 1000-fold, but the RT-PCR

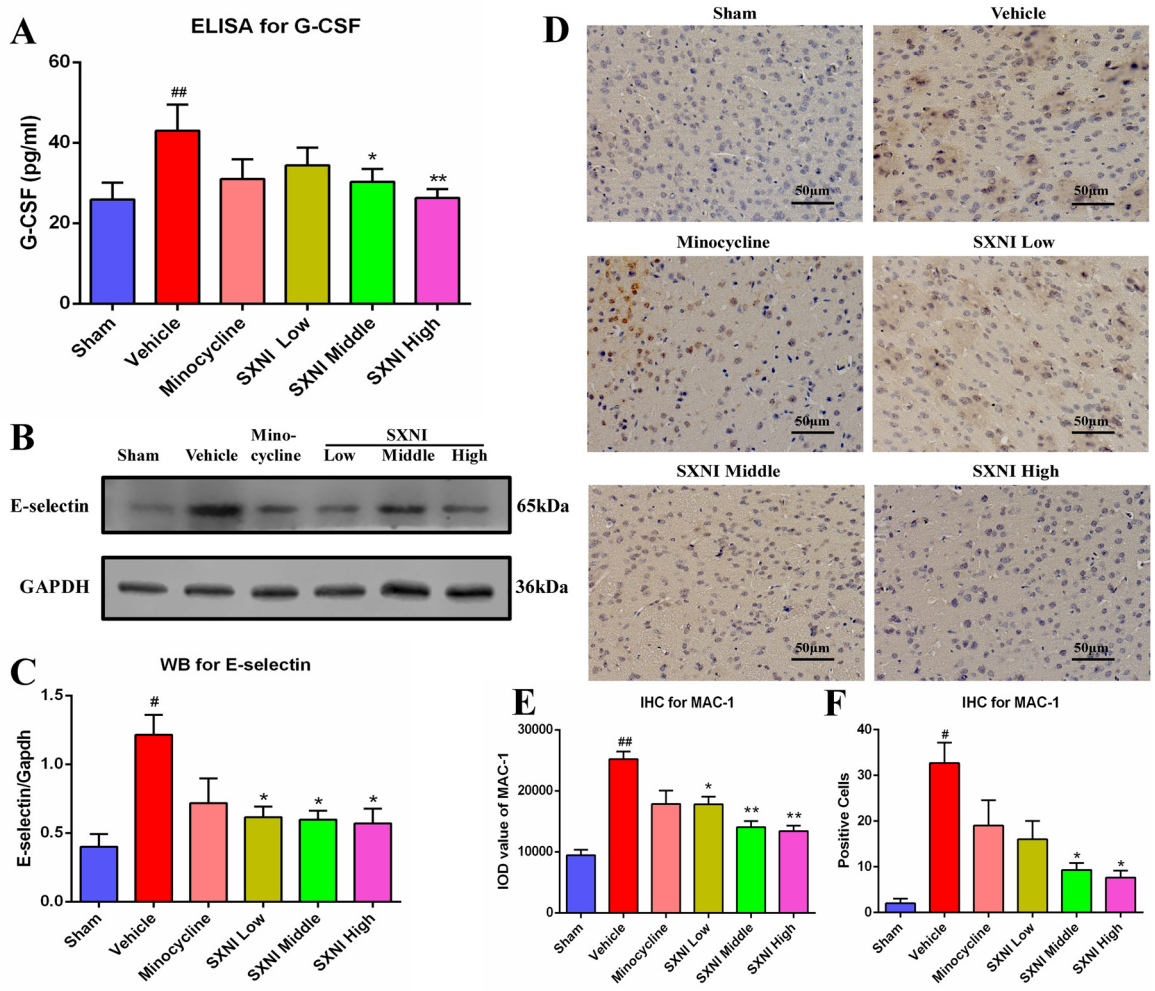

Fig. 8. Determination of G-CSF, E-selectin, MAC-1 protein expression in serum and brain tissue. (A) Effect of SXNI on G-CSF protein expression in serum of subacute stroke mice (n = 6). (B) Representative western blot images of E-selectin protein expression in brain tissue after different treatment. (C) Quantification of western-blot results of E-selectin protein (n = 3 for each group). (D) Immunohistochemical staining results of MAC-1 protein in brain tissue sections (40× magnification). (E) Quantification of immunohistochemical staining results of MAC-1 protein in brain tissue sections after different treatment (n = 3 for each group). Data were expressed as mean ± SD. $^{\#}P < 0.05$, $^{\#\#}P < 0.01$ vs. Sham group, $^{*}P < 0.05$, $^{**}P < 0.01$ vs. Vehicle group.

validation showed only about 4-fold change (Fig. 6G vs. Fig. 7B), whereas the difference in the expression of G-CSF protein detected in the serum of mice in the SXNI and vehicle groups was even less (Fig. 8A). These apparent disparity may be attributed to the methodological sensitivity as well as selective expression of genes in different cells and tissues [111]. In addition, although exogenous G-CSF has been reported to have a neuroprotective effect on stroke mice, no significant effect has been achieved in clinical trials and meta-analyses [112,113]. From the above, G-CSF may play a dual role in the immune/inflammatory response [114,115].

Although our experiments showed that SXNI can inhibit granulocyte adhesion and diapedesis via down-regulating the expression of G-CSF, E-selectin and MAC-1, thereby improving brain damage and restoring neuromotor functions in subacute stroke mice, there are still some limitations to the work. For example, (1) To avoid the effect of estrogens on brain protection, only male mice were selected in this study. (2) the effect on granulocyte migration has not been functionally verified; (3) whether our model of “post-stroke recovery” corresponds to the human clinical case needs confirmation; (4) except for the acute and subacute of stroke, other longer period models for stroke recovery are being established. The common and differential mechanisms of SXNI in different stages of protection and treatment of stroke will also be further explored. In summary, our study showed that SXNI, an effective ginkgo biloba extract, can contribute to improve brain damage and restore neuromotor function in subacute stroke mice.

5. Conclusion

Our research first indicate that SXNI can improve the brain damage and neurological recovery of stroke mice via inhibiting the expression of G-CSF, E-selectin and MAC-1 proteins, which may be related to down-regulation of granulocyte adhesion and diapedesis pathway. In addition, the high expression of inflammatory mediators and adhesion molecules associated with this pathway can also be significantly down-regulated by SXNI Overall, this study mode some contributions to treating neurological recovery of subacute stroke, and provided experimental basis for clinical application of SXNI.

Author contributions

YZ conceived the research theme and supervised its implementation. ZL and GX completed the relevant experiments of Figs. 1, 3, 4 and 8. ML analyzed the data using IPA and provided Fig. 6. ZL and YW participated in the Catwalk experiment in Fig. 2. ZL, SH, HD and XW performed RT-PCR experiments and depicted Fig. 7. YF discussed the experimental design. YZ, ZL and GX wrote the manuscript. All authors

reviewed and approved the manuscript.

Funding

This study was supported by funds from National Natural Science Foundation of China (81873037) and the Major National Science and Technology Projects of China (2018YFC1704502), which are used for purchasing reagents and experimental animals, maintaining laboratory instruments and part of personnel costs. The funding body did not play a role in the study design, performance, data collection and analysis, decision to publish, or preparation/writing of the manuscript.

Declaration of Competing Interest

The authors declare that this research was conducted without any commercial or financial relationship, which could be interpreted as a potential conflict of interest.

Acknowledgements

We would like to thank our lab members, particularly Drs. Jian Yang, Pengzhi Dong, Rui Shao, Ying Cui and John Owoicho Orgah, for stimulating discussion and sharing of reagents.

Appendix A. Supplementary data

Supplementary material related to this article can be found, in the online version, at doi:https://doi.org/10.1016/j.biopha.2020.110213.

References

[1] W. Wang, B. Jiang, H. Sun, X. Ru, D. Sun, L. Wang, L. Wang, Y. Jiang, Y. Li, Y. Wang, et al., Prevalence, incidence, and mortality of stroke in China: results from a nationwide population-based survey of 480 687 adults, Circulation 135 (8) (2017) 759–771, https://doi.org/10.1161/CIRCULATIONAHA.116.025250.

[2] M.S. Ekker, J.I. Verhoeven, I. Vaartjes, W.M.T. Jolink, C.J.M. Klijn, F.E. de Leeuw, Association of stroke among adults aged 18 to 49 years with long-term mortality, JAMA 321 (21) (2019) 2113–2123, https://doi.org/10.1001/jama.2019.6560.

[3] E.J. Benjamin, S.S. Virani, C.W. Callaway, A.M. Chamberlain, A.R. Chang, S. Cheng, S.E. Chiuve, M. Cushman, F.N. Delling, R. Deo, et al., Heart disease and stroke statistics-2018 update: a report from the American Heart Association, Circulation 137 (12) (2018) e67–e492, https://doi.org/10.1161/CIR.0000000000000558.

[4] M. McManus, D.S. Liebeskind, Blood pressure in acute ischemic stroke, J. Clin. Neurol. 12 (2) (2016) 137–146, https://doi.org/10.3988/jcn.2016.12.2.137.

[5] R. Dubinsky, Lai SM, Mortality of stroke patients treated with thrombolysis: analysis of nationwide inpatient sample, Neurology 66 (11) (2006) 1742–1744, https://doi.org/10.1212/01.wnl.0000218306.35681.38.

[6] C.R. Cassella, A. Jagoda, Ischemic stroke: advances in diagnosis and management, Emerg. Med. Clin. North Am. 35 (4) (2017) 911–930.

[7] H.B. van der Worp, J. van Gijn, Clinical practice. Acute ischemic stroke, N. Engl. J. Med. 357 (6) (2007) 572–579, https://doi.org/10.1056/NEJMcp072057.

[8] C.A. Cronin, K.N. Sheth, X. Zhao, S.R. Messé, D.M. Olson, A.F. Hernandez, D.L. Bhatt, L.H. Schwamm, E.E. Smith, Adherence to Third European Cooperative Acute Stroke Study 3- to 4.5-hour exclusions and association with outcome: data from get with the Guidelines-Stroke, Stroke 45 (9) (2014) 2745–2749, https://doi.org/10.1161/STROKEAHA.114.005443.

[9] S.R. Levine, P. Khatri, J.P. Broderick, J.C. Grotta, S.E. Kasner, D. Kim, B.C. Meyer, P. Panagos, J. Romano, P. Scott, Review, historical context, and clarifications of the NINDS rt-PA stroke trials exclusion criteria: part 1: rapidly improving stroke symptoms, Stroke 44 (9) (2013) 2500–2505, https://doi.org/10.1161/STROKEAHA.113.000878.

[10] S.C. Cramer, M. Chopp, Recovery recapitulates ontogeny, Trends Neurosci. 23 (6) (2000) 265–271, https://doi.org/10.1016/s0166-2236(00)01562-9.

[11] M. Goyal, B.K. Menon, W.H. van Zwam, D.W. Dippel, P.J. Mitchell, A.M. Demchuk, A. Davalos, C.B. Majoie, A. van der Lugt, M.A. de Miquel, et al., Endovascular thrombectomy after large-vessel ischaemic stroke: a meta-analysis of individual patient data from five randomised trials, Lancet 387 (10029) (2016) 1723–1731, https://doi.org/10.1016/S0140-6736(16)00163-X.

[12] T.G. Jovin, A. Chamorro, E. Cobo, M.A. de Miquel, C.A. Molina, A. Rovira, L. San Roman, J. Serena, S. Abilleira, M. Ribo, et al., Thrombectomy within 8 hours after symptom onset in ischemic stroke, N. Engl. J. Med. 372 (24) (2015) 2296–2306, https://doi.org/10.1056/NEJMoa1503780.

[13] M. Goyal, A.M. Demchuk, B.K. Menon, M. Eesa, J.L. Rempel, J. Thornton, D. Roy, T.G. Jovin, R.A. Willinsky, B.L. Sapkota, et al., Randomized assessment of rapid endovascular treatment of ischemic stroke, N. Engl. J. Med. 372 (11) (2015) 1019–1030, https://doi.org/10.1056/NEJMoa1414905.

[14] J.M. Kim, J.H. Bae, K.Y. Park, W.J. Lee, J.S. Byun, S.W. Ahn, H.W. Shin, S.H. Han, I.H. Yoo, Incidence and mechanism of early neurological deterioration after endovascular thrombectomy, J. Neurol. 266 (3) (2019) 609–615, https://doi.org/10.1007/s00415-018-09173-0.

[15] R.L. Zhang, M. Chopp, H. Chen, J.H. Garcia, Temporal profile of ischemic tissue damage, neutrophil response, and vascular plugging following permanent and transient (2H) middle cerebral artery occlusion in the rat, J. Neurol. Sci. 125 (1) (1994) 3–10, https://doi.org/10.1016/0022-510x(94)90234-8.

[16] H.L. Schimidt, A. Vieira, C. Altermann, A. Martins, P. Sosa, F.W. Santos, P.B. Mello-Carpes, I. Izquierdo, F.P. Carpes, Memory deficits and oxidative stress in cerebral ischemia-reperfusion: neuroprotective role of physical exercise and green tea supplementation, Neurobiol. Learn. Mem. 114 (2014) 242–250, https://doi.org/10.1016/j.nlm.2014.07.005.

[17] P. Jhelum, A.B. Wahul, A. Kamle, S. Kumawat, A. Kumar, K.K. Bhutani, S.M. Tripathi, S. Chakravarty, Sameerpannag Ras Mixture (SRM) improved neurobehavioral deficits following acute ischemic stroke by attenuating neuroinflammatory response, J. Ethnopharmacol. 197 (2017) 147–156, https://doi.org/10.1016/j.jep.2016.07.059.

[18] S.H. Koh, H.H. Park, Neurogenesis in stroke recovery, Transl. Stroke Res. 8 (1) (2017) 3–13, https://doi.org/10.1007/s12975-016-0460-z.

[19] D.J. Gladstone, S.E. Black, A.M. Hakim, Heart, Stroke Foundation of Ontario Centre of Excellence in Stroke R: toward wisdom from failure: lessons from neuroprotective stroke trials and new therapeutic directions, Stroke 33 (8) (2002) 2123–2136, https://doi.org/10.1161/01.str.0000025518.34157.51.

[20] G.C. Jickling, F.R. Sharp, Improving the translation of animal ischemic stroke studies to humans, Metab. Brain Dis. 30 (2) (2015) 461–467, https://doi.org/10.1007/s11011-014-9499-2.

[21] F. Fluri, M.K. Schuhmann, C. Kleinschnitz, Animal models of ischemic stroke and their application in clinical research, Drug Des. Devel. Ther. 9 (2015) 3445–3454, https://doi.org/10.2147/DDDT.S56071.

[22] A. Kumar, Aakriti, V. Gupta, A review on animal models of stroke: An update, Brain Res. Bull. 122 (2016) 35–44, https://doi.org/10.1016/j.brainresbull.2016.02.016.

[23] M. Fisher, G. Feuerstein, D.W. Howells, P.D. Hurn, T.A. Kent, S.I. Savitz, E.H. Lo, Update of the stroke therapy academic industry roundtable preclinical recommendations, Stroke 40 (6) (2009) 2244–2250, https://doi.org/10.1161/STROKEAHA.108.541128.

[24] T.S. Olsen, E.B. Skriver, M. Herning, Cause of cerebral infarction in the carotid territory. Its relation to the size and the location of the infarct and to the underlying vascular lesion, Stroke 16 (3) (1985) 459–466.

[25] C.J. Sommer, Ischemic stroke: experimental models and reality, Acta Neuropathol. 133 (2) (2017) 245–261, https://doi.org/10.1007/s00401-017-1667-0.

[26] A.A. Neuhaus, T. Rabie, B.A. Sutherland, M. Papadakis, G. Hadley, R. Cai, A.M. Buchan, Importance of preclinical research in the development of neuroprotective strategies for ischemic stroke, JAMA Neurol. 71 (5) (2014) 634–639.

[27] M. Lyu, Y. Cui, T. Zhao, Z. Ning, J. Ren, X. Jin, G. Fan, Y. Zhu, Tnfrsf12a-mediated atherosclerosis signaling and inflammatory response as a common protection mechanism of shuxuening injection against both myocardial and cerebral ischemia-reperfusion injuries, Front. Pharmacol. 9 (2018) 312, https://doi.org/10.3389/fphar.2018.00312.

[28] G. Xiao, M. Lyu, Y. Wang, S. He, X. Liu, J. Ni, L. Li, G. Fan, J. Han, X. Gao, et al., Ginkgo flavonol glycosides or ginkgolides tend to differentially protect myocardial or cerebral ischemia-reperfusion injury regulation of TWEAK-Fn14 signaling in heart and brain, Front. Pharmacol. 10 (2019) 735, https://doi.org/10.3389/fphar.2019.00735.

[29] H. Xie, J.-R. Wang, L.-F. Yau, Y. Liu, L. Liu, Q.-B. Han, Z. Zhao, Z.-H. Jiang, Quantitative analysis of the flavonoid glycosides and terpene trilactones in the extract of Ginkgo biloba and evaluation of their inhibitory activity towards fibril formation of β-amyloid peptide, Molecules 19 (4) (2014) 4466–4478, https://doi.org/10.3390/molecules19044466.

[30] T.A. van Beek, P. Montoro, Chemical analysis and quality control of Ginkgo biloba leaves, extracts, and phytopharmaceuticals, J. Chromatogr. A 1216 (11) (2009) 2002–2032, https://doi.org/10.1016/j.chroma.2009.01.013.

[31] C. Ude, M. Schubert-Zsilavecz, M. Wurglics, Ginkgo biloba extracts: a review of the pharmacokinetics of the active ingredients, Clin. Pharmacokinet. 52 (9) (2013) 727–749, https://doi.org/10.1007/s40262-013-0074-5.

[32] B. Ahlemeyer, J. Krieglstein, Neuroprotective effects of Ginkgo biloba extract, Cell. Mol. Life Sci. 60 (9) (2003) 1779–1792.

[33] S.E. Nada, J. Tulsulkar, Z.A. Shah, Heme oxygenase 1-mediated neurogenesis is enhanced by Ginkgo biloba (EGb 761(R)) after permanent ischemic stroke in mice, Mol. Neurobiol. 49 (2) (2014) 945–956, https://doi.org/10.1007/s12035-013-8572-x.

[34] Y. Zhang, J. Liu, B. Yang, Y. Zheng, M. Yao, M. Sun, L. Xu, C. Lin, D. Chang, F. Tian, Ginkgo biloba extract inhibits astrocytic Lipocalin-2 expression and alleviates neuroinflammatory injury via the JAK2/STAT3 pathway after ischemic brain stroke, Front. Pharmacol. 9 (2018) 518, https://doi.org/10.3389/fphar.2018.00518.

[35] B. Yin, H. Liang, Y. Chen, K. Chu, L. Huang, L. Fang, E. Matro, W. Jiang, B. Luo, EGB1212 post-treatment ameliorates hippocampal CA1 neuronal death and memory impairment induced by transient global cerebral ischemia/reperfusion, Am. J. Chin. Med. (Gard City N Y) 41 (6) (2013) 1329–1341, https://doi.org/10.1142/S0192415X13500894.

[36] Z.F. Guan, X.M. Zhang, Y.H. Tao, Y. Zhang, Y.Y. Huang, G. Chen, W.J. Tang, G. Ji, Q.L. Guo, M. Liu, et al., EGb761 improves the cognitive function of elderly db/db (-/-) diabetic mice by regulating the beclin-1 and NF-kappaB signaling pathways,

Metab. Brain Dis. 33 (6) (2018) 1887–1897, https://doi.org/10.1007/s11011-018-0295-2.
[37] S.L. Harms, J. Garrard, P. Schwinghammer, L.E. Eberly, Y. Chang, I.E. Leppik, Ginkgo biloba use in nursing home elderly with epilepsy or seizure disorder, Epilepsia 47 (2) (2006) 323–329, https://doi.org/10.1111/j.1528-1167.2006.00424.x.
[38] A.G. Mazumder, P. Sharma, V. Patial, D. Singh, Ginkgo biloba L. attenuates spontaneous recurrent seizures and associated neurological conditions in lithium-pilocarpine rat model of temporal lobe epilepsy through inhibition of mammalian target of rapamycin pathway hyperactivation, J. Ethnopharmacol. 204 (2017) 8–17, https://doi.org/10.1016/j.jep.2017.03.060.
[39] C. Shi, J. Liu, F. Wu, D.T. Yew, Ginkgo biloba extract in Alzheimer's disease: from action mechanisms to medical practice, Int. J. Mol. Sci. 11 (1) (2010) 107–123, https://doi.org/10.3390/ijms11010107.
[40] N. Kandiah, P.A. Ong, T. Yuda, L.L. Ng, K. Mamun, R.A. Merchant, C. Chen, J. Dominguez, S. Marasigan, E. Ampil, et al., Treatment of dementia and mild cognitive impairment with or without cerebrovascular disease: expert consensus on the use of Ginkgo biloba extract, EGb 761((R)), CNS Neurosci. Ther. 25 (2) (2019) 288–298, https://doi.org/10.1111/cns.13095.
[41] B. Vellas, N. Coley, P.J. Ousset, G. Berrut, J.F. Dartigues, B. Dubois, H. Grandjean, F. Pasquier, F. Piette, P. Robert, et al., Long-term use of standardised Ginkgo biloba extract for the prevention of Alzheimer's disease (GuidAge): a randomised placebo-controlled trial, Lancet Neurol. 11 (10) (2012) 851–859, https://doi.org/10.1016/S1474-4422(12)70206-5.
[42] G.R. Zeng, S.D. Zhou, Y.J. Shao, M.H. Zhang, L.M. Dong, J.W. Lv, M.H.X. Zhang, Y.H. Tang, D.J. Jiang, X.M. Liu, Effect of Ginkgo biloba extract-761 on motor functions in permanent middle cerebral artery occlusion rats, Phytomedicine 48 (2018) 94–103, https://doi.org/10.1016/j.phymed.2018.05.003.
[43] S. Li, X. Zhang, Q. Fang, J. Zhou, M. Zhang, H. Wang, Y. Chen, B. Xu, Y. Wu, L. Qian, et al., Ginkgo biloba extract improved cognitive and neurological functions of acute ischaemic stroke: a randomised controlled trial, Stroke Vasc. Neurol. 2 (4) (2017) 189–197, https://doi.org/10.1136/svn-2017-000104.
[44] H. Ma, J. Li, M. An, X.M. Gao, Y.X. Chang, A powerful on line ABTS(+)-CE-DAD method to screen and quantify major antioxidants for quality control of Shuxuening Injection, Sci. Rep. 8 (1) (2018) 5441, https://doi.org/10.1038/s41598-018-23748-x.
[45] H.F. Elewa, H. Hilali, D.C. Hess, L.S. Machado, S.C. Fagan, Minocycline for short-term neuroprotection, Pharmacotherapy 26 (4) (2006) 515–521, https://doi.org/10.1592/phco.26.4.515.
[46] W.P. Yew, N.D. Djukic, J.S.P. Jayaseelan, F.R. Walker, K.A.A. Roos, T.K. Chataway, H. Muyderman, N.R. Sims, Early treatment with minocycline following stroke in rats improves functional recovery and differentially modifies responses of peri-infarct microglia and astrocytes, J. Neuroinflammation 16 (1) (2019) 6, https://doi.org/10.1186/s12974-018-1379-y.
[47] K. Malhotra, J.J. Chang, A. Khunger, D. Blacker, J.A. Switzer, N. Goyal, A.V. Hernandez, V. Pasupuleti, A.V. Alexandrov, G. Tsivgoulis, Minocycline for acute stroke treatment: a systematic review and meta-analysis of randomized clinical trials, J. Neurol. 265 (8) (2018) 1871–1879, https://doi.org/10.1007/s00415-018-8935-3.
[48] D. Petrovic-Djergovic, S.N. Goonewardena, D.J. Pinsky, Inflammatory disequilibrium in stroke, Circ. Res. 119 (1) (2016) 142–158, https://doi.org/10.1161/CIRCRESAHA.116.308022.
[49] B. Li, K. Concepcion, X. Meng, L. Zhang, Brain-immune interactions in perinatal hypoxic-ischemic brain injury, Prog. Neurobiol. 159 (2017) 50–68, https://doi.org/10.1016/j.pneurobio.2017.10.006.
[50] A. Breedveld, T. Groot Kormelink, M. van Egmond, E.C. de Jong, Granulocytes as modulators of dendritic cell function, J. Leukoc. Biol. 102 (4) (2017) 1003–1016, https://doi.org/10.1189/jlb.4MR0217-048RR.
[51] T. Peng, W. Wan, J. Wang, Y. Liu, Z. Fu, X. Ma, J. Li, G. Sun, Y. Ji, J. Lu, et al., The neurovascular protective effect of S14G-Humanin in a murine MCAO model and brain endothelial cells, IUBMB Life 70 (7) (2018) 691–699, https://doi.org/10.1002/iub.1869.
[52] W. Luo, H. Wang, M.K. Ohman, C. Guo, K. Shi, J. Wang, D.T. Eitzman, P-selectin glycoprotein ligand-1 deficiency leads to cytokine resistance and protection against atherosclerosis in apolipoprotein E deficient mice, Atherosclerosis 220 (1) (2012) 110–117, https://doi.org/10.1016/j.atherosclerosis.2011.10.012.
[53] H. Wang, L.J. Hong, J.Y. Huang, Q. Jiang, R.R. Tao, C. Tan, N.N. Lu, C.K. Wang, M.M. Ahmed, Y.M. Lu, et al., P2RX7 sensitizes Mac-1/ICAM-1-dependent leukocyte-endothelial adhesion and promotes neurovascular injury during septic encephalopathy, Cell Res. 25 (6) (2015) 674–690, https://doi.org/10.1038/cr.2015.61.
[54] W.A. Muller, Getting leukocytes to the site of inflammation, Vet. Pathol. 50 (1) (2013) 7–22, https://doi.org/10.1177/0300985812469883.
[55] B. Rossi, S. Angiari, E. Zenaro, S.L. Budui, G. Constantin, Vascular inflammation in central nervous system diseases: adhesion receptors controlling leukocyte-endothelial interactions, J. Leukoc. Biol. 89 (4) (2011) 539–556, https://doi.org/10.1189/jlb.0710432.
[56] X. Chen, S.E. Kelemen, M.V. Autieri, Expression of granulocyte colony-stimulating factor is induced in injured rat carotid arteries and mediates vascular smooth muscle cell migration, Am. J. Physiol., Cell Physiol. 288 (1) (2005) C81–C88.
[57] G.D. Demetri, J.D. Griffin, Granulocyte colony-stimulating factor and its receptor, Blood 78 (11) (1991) 2791–2808.
[58] J. Neumanaitis, Granulocyte-macrophage-colony-stimulating factor: a review from preclinical development to clinical application, Transfusion 33 (1) (1993) 70–83, https://doi.org/10.1046/j.1537-2995.1993.33193142315.x.
[59] G. Carulli, Effects of recombinant human granulocyte colony-stimulating factor administration on neutrophil phenotype and functions, Haematologica 82 (5) (1997) 606–616.
[60] I.K. Campbell, U. Novak, J. Cebon, J.E. Layton, J.A. Hamilton, Human articular cartilage and chondrocytes produce hemopoietic colony-stimulating factors in culture in response to IL-1, J. Immunol. 147 (4) (1991) 1238–1246.
[61] A.W. Roberts, G-CSF: a key regulator of neutrophil production, but that's not all!, Growth Factors 23 (1) (2005) 33–41.
[62] J.L. Eyles, M.J. Hickey, M.U. Norman, B.A. Croker, A.W. Roberts, S.F. Drake, W.G. James, D. Metcalf, I.K. Campbell, I.P. Wicks, A key role for G-CSF-induced neutrophil production and trafficking during inflammatory arthritis, Blood 112 (13) (2008) 5193–5201, https://doi.org/10.1182/blood-2008-02-139535.
[63] I.K. Campbell, M.J. Rich, R.J. Bischof, J.A. Hamilton, The colony-stimulating factors and collagen-induced arthritis: exacerbation of disease by M-CSF and G-CSF and requirement for endogenous M-CSF, J. Leukoc. Biol. 68 (1) (2000) 144–150.
[64] A. Taguchi, Z. Wen, K. Myojin, T. Yoshihara, T. Nakagomi, D. Nakayama, H. Tanaka, T. Soma, D.M. Stern, H. Naritomi, et al., Granulocyte colony-stimulating factor has a negative effect on stroke outcome in a murine model, Eur. J. Neurosci. 26 (1) (2007) 126–133.
[65] A.D. Christensen, C. Haase, A.D. Cook, J.A. Hamilton, Granulocyte colony-stimulating factor (G-CSF) plays an important role in immune complex-mediated arthritis, Eur. J. Immunol. 46 (5) (2016) 1235–1245, https://doi.org/10.1002/eji.201546185.
[66] J.L. Eyles, A.W. Roberts, D. Metcalf, I.P. Wicks, Granulocyte colony-stimulating factor and neutrophils–forgotten mediators of inflammatory disease, Nat. Clin. Pract. Rheumatol. 2 (9) (2006) 500–510, https://doi.org/10.1038/ncprheum0291.
[67] M. Eberle, P. Ebel, C.A. Mayer, J. Barthelmes, N. Tafferner, N. Ferreiros, T. Ulshöfer, M. Henke, C. Foerch, A.M. de Bazo, et al., Exacerbation of experimental autoimmune encephalomyelitis in ceramide synthase 6 knockout mice is associated with enhanced activation/migration of neutrophils, Immunol. Cell Biol. 93 (9) (2015) 825–836, https://doi.org/10.1038/icb.2015.47.
[68] A. Ohsaka, K. Saionji, J. Igari, Granulocyte colony-stimulating factor administration increases serum concentrations of soluble selectins, Br. J. Haematol. 100 (1) (1998) 66–69, https://doi.org/10.1046/j.1365-2141.1998.00510.x.
[69] N.M. Dagia, S.Z. Gadhoum, C.A. Knoblauch, J.A. Spencer, P. Zamiri, C.P. Lin, R. Sackstein, G-CSF induces E-selectin ligand expression on human myeloid cells, Nat. Med. 12 (10) (2006) 1185–1190.
[70] C.I. Silvescu, R. Sackstein, G-CSF induces membrane expression of a myeloperoxidase glycovariant that operates as an E-selectin ligand on human myeloid cells, Proc. Natl. Acad. Sci. U. S. A. 111 (29) (2014) 10696–10701, https://doi.org/10.1073/pnas.1320833111.
[71] B. Fusté, R. Mazzara, G. Escolar, A. Merino, A. Ordinas, M. Díaz-Ricart, Granulocyte colony-stimulating factor increases expression of adhesion receptors on endothelial cells through activation of p38 MAPK, Haematologica 89 (5) (2004) 578–585.
[72] Y. Li, M. Chopp, J. Chen, L. Wang, S.C. Gautam, Y.X. Xu, Z. Zhang, Intrastriatal transplantation of bone marrow nonhematopoietic cells improves functional recovery after stroke in adult mice, J. Cereb. Blood Flow Metab. 20 (9) (2000) 1311–1319.
[73] J. Chen, C. Zhang, H. Jiang, Y. Li, L. Zhang, A. Robin, M. Katakowski, M. Lu, M. Chopp, Atorvastatin induction of VEGF and BDNF promotes brain plasticity after stroke in mice, J. Cereb. Blood Flow Metab. 25 (2) (2005) 281–290, https://doi.org/10.1038/sj.jcbfm.9600034.
[74] M.J. Glenn, E.D. Kirby, E.M. Gibson, S.J. Wong-Goodrich, T.J. Mellott, J.K. Blusztajn, C.L. Williams, Age-related declines in exploratory behavior and markers of hippocampal plasticity are attenuated by prenatal choline supplementation in rats, Brain Res. 1237 (2008) 110–123, https://doi.org/10.1016/j.brainres.2008.08.049.
[75] H.L. Sanchez, L.B. Silva, E.L. Portiansky, C.B. Herenu, R.G. Goya, G.O. Zuccolilli, Dopaminergic mesencephalic systems and behavioral performance in very old rats, Neuroscience 154 (4) (2008) 1598–1606, https://doi.org/10.1016/j.neuroscience.2008.04.016.
[76] E. Caballero-Garrido, J.C. Pena-Philippides, Z. Galochkina, E. Erhardt, T. Roitbak, Characterization of long-term gait deficits in mouse dMCAO, using the CatWalk system, Behav. Brain Res. 331 (2017) 282–296, https://doi.org/10.1016/j.bbr.2017.05.042.
[77] S. Parkkinen, F.J. Ortega, K. Kuptsova, J. Huttunen, I. Tarkka, J. Jolkkonen, Gait impairment in a rat model of focal cerebral ischemia, Stroke Res. Treat. 2013 (2013) 410972, , https://doi.org/10.1155/2013/410972.
[78] L. Qin, D. Jing, S. Parauda, J. Carmel, R.R. Ratan, F.S. Lee, S. Cho, An adaptive role for BDNF Val66Met polymorphism in motor recovery in chronic stroke, J. Neurosci. 34 (7) (2014) 2493–2502, https://doi.org/10.1523/JNEUROSCI.4140-13.2014.
[79] N.W. Liu, C.C. Ke, Y. Zhao, Y.A. Chen, K.C. Chan, D.T. Tan, J.S. Lee, Y.A. Chen, T.W. Hsu, Y.J. Hsieh, et al., Evolutional characterization of photochemically induced stroke in rats: a multimodality imaging and molecular biological study, Transl. Stroke Res. 8 (3) (2017) 244–256, https://doi.org/10.1007/s12975-016-0512-4.
[80] D.W. McBride, D. Klebe, J. Tang, J.H. Zhang, Correcting for brain swelling's effects on infarct volume calculation after middle cerebral artery occlusion in rats, Transl. Stroke Res. 6 (4) (2015) 323–338, https://doi.org/10.1007/s12975-015-0400-3.
[81] J.Y. Park, S.K. Lee, J.Y. Kim, K.H. Je, D. Schellingerhout, D.E. Kim, A new micro-computed tomography-based high-resolution blood-brain barrier imaging technique to study ischemic stroke, Stroke 45 (8) (2014) 2480–2484, https://doi.org/10.1161/STROKEAHA.114.006297.

[82] T.H. Murphy, D. Corbett, Plasticity during stroke recovery: from synapse to behaviour, Nat. Rev. Neurosci. 10 (12) (2009) 861–872, https://doi.org/10.1038/nrn2735.
[83] D. Corbett, S.T. Carmichael, T.H. Murphy, T.A. Jones, M.E. Schwab, J. Jolkkonen, A.N. Clarkson, N. Dancause, T. Weiloch, H. Johansen-Berg, et al., Enhancing the alignment of the preclinical and clinical stroke recovery research pipeline: consensus-based core recommendations from the stroke recovery and rehabilitation roundtable translational working group, Neurorehabil. Neural Repair 31 (8) (2017) 699–707, https://doi.org/10.1177/1545968317724285.
[84] H.M. Finestone, L.S. Greene-Finestone, Rehabilitation medicine: 2. Diagnosis of dysphagia and its nutritional management for stroke patients, CMAJ 169 (10) (2003) 1041–1044.
[85] A. Westergren, S. Karlsson, P. Andersson, O. Ohlsson, I.R. Hallberg, Eating difficulties, need for assisted eating, nutritional status and pressure ulcers in patients admitted for stroke rehabilitation, J. Clin. Nurs. 10 (2) (2001) 257–269.
[86] A.G. Thrift, T. Thayabaranathan, G. Howard, V.J. Howard, P.M. Rothwell, V.L. Feigin, B. Norrving, G.A. Donnan, D.A. Cadilhac, Global stroke statistics, Int. J. Stroke 12 (1) (2017) 13–32, https://doi.org/10.1177/1747493016676285.
[87] P. Xu, Q. Liu, Y. Xie, X. Shi, Y. Li, M. Peng, H. Guo, R. Sun, J. Li, Y. Hong, et al., Breast cancer susceptibility protein 1 (BRCA1) rescues neurons from cerebral ischemia/reperfusion injury through NRF2-mediated antioxidant pathway, Redox Biol. 18 (2018) 158–172, https://doi.org/10.1016/j.redox.2018.06.012.
[88] B. Manwani, F. Liu, Y. Xu, R. Persky, J. Li, L.D. McCullough, Functional recovery in aging mice after experimental stroke, Brain Behav. Immun. 25 (8) (2011) 1689–1700, https://doi.org/10.1016/j.bbi.2011.06.015.
[89] W. Zuo, P.F. Yang, J. Chen, Z. Zhang, N.H. Chen, Drp-1, a potential therapeutic target for brain ischaemic stroke, Br. J. Pharmacol. 173 (10) (2016) 1665–1677, https://doi.org/10.1111/bph.13468.
[90] C. Vandeputte, J.M. Taymans, C. Casteels, F. Coun, Y. Ni, K. Van Laere, V. Baekelandt, Automated quantitative gait analysis in animal models of movement disorders, BMC Neurosci. 11 (2010) 92, https://doi.org/10.1186/1471-2202-11-92.
[91] F. Fluri, U. Malzahn, G.A. Homola, M.K. Schuhmann, C. Kleinschnitz, J. Volkmann, Stimulation of the mesencephalic locomotor region for gait recovery after stroke, Ann. Neurol. 82 (5) (2017) 828–840, https://doi.org/10.1002/ana.25086.
[92] S. Hetze, C. Römer, C. Teufelhart, A. Meisel, O. Engel, Gait analysis as a method for assessing neurological outcome in a mouse model of stroke, J. Neurosci. Methods 206 (1) (2012), https://doi.org/10.1016/j.jneumeth.2012.02.001.
[93] S. Nourshargh, R. Alon, Leukocyte migration into inflamed tissues, Immunity 41 (5) (2014) 694–707, https://doi.org/10.1016/j.immuni.2014.10.008.
[94] M.G. Tonnesen, Neutrophil-endothelial cell interactions: mechanisms of neutrophil adherence to vascular endothelium, J. Invest. Dermatol. 93 (Suppl. 2) (1989) 53S–58S, https://doi.org/10.1111/1523-1747.ep12581069.
[95] S.L. Maas, O. Soehnlein, J.R. Viola, Organ-specific mechanisms of transendothelial neutrophil migration in the lung, liver, kidney, and aorta, Front. Immunol. 9 (2018) 2739, https://doi.org/10.3389/fimmu.2018.02739.
[96] P.K. Jani, E. Schwaner, E. Kajdacsi, M.L. Debreczeni, R. Ungai-Salanki, J. Dobo, Z. Doleschall, J. Rigo Jr., M. Geiszt, B. Szabo, et al., Complement MASP-1 enhances adhesion between endothelial cells and neutrophils by up-regulating E-selectin expression, Mol. Immunol. 75 (2016) 38–47, https://doi.org/10.1016/j.molimm.2016.05.007.
[97] Y. Su, X. Lei, L. Wu, Liu L, The role of endothelial cell adhesion molecules P-selectin, E-selectin and intercellular adhesion molecule-1 in leucocyte recruitment induced by exogenous methylglyoxal, Immunology 137 (1) (2012) 65–79, https://doi.org/10.1111/j.1365-2567.2012.03608.x.
[98] K.L. Moore, K.D. Patel, R.E. Bruehl, F. Li, D.A. Johnson, H.S. Lichenstein, R.D. Cummings, D.F. Bainton, R.P. McEver, P-selectin glycoprotein ligand-1 mediates rolling of human neutrophils on P-selectin, J. Cell Biol. 128 (4) (1995) 661–671, https://doi.org/10.1083/jcb.128.4.661.
[99] M.K. Wild, M.C. Huang, U. Schulze-Horsel, P.A. van der Merwe, D. Vestweber, Affinity, kinetics, and thermodynamics of E-selectin binding to E-selectin ligand-1, J. Biol. Chem. 276 (34) (2001) 31602–31612, https://doi.org/10.1074/jbc.M104844200.
[100] E. Mordelet, H.A. Davies, P. Hillyer, I.A. Romero, D. Male, Chemokine transport across human vascular endothelial cells, Endothelium 14 (1) (2007) 7–15, https://doi.org/10.1080/10623320601177312.
[101] E.A. Subileau, P. Rezaie, H.A. Davies, F.M. Colyer, J. Greenwood, D.K. Male, I.A. Romero, Expression of chemokines and their receptors by human brain endothelium: implications for multiple sclerosis, J. Neuropathol. Exp. Neurol. 68 (3) (2009) 227–240, https://doi.org/10.1097/NEN.0b013e318197eca7.
[102] D.W. Wojkowska, P. Szpakowski, A. Glabinski, Interleukin 17A promotes lymphocytes adhesion and induces CCL2 and CXCL1 release from brain endothelial cells, Int. J. Mol. Sci. 18 (5) (2017), https://doi.org/10.3390/ijms18051000.
[103] K. Thamm, S. Graupner, C. Werner, W.B. Huttner, D. Corbeil, Monoclonal antibodies 13A4 and AC133 do not recognize the canine ortholog of mouse and human stem cell antigen Prominin-1 (CD133), PLoS One 11 (10) (2016) e0164079, , https://doi.org/10.1371/journal.pone.0164079.
[104] K. Futosi, S. Fodor, A. Mocsai, Reprint of Neutrophil cell surface receptors and their intracellular signal transduction pathways, Int. Immunopharmacol. 17 (4) (2013) 1185–1197, https://doi.org/10.1016/j.intimp.2013.11.010.
[105] C.W. Smith, S.D. Marlin, R. Rothlein, C. Toman, D.C. Anderson, Cooperative interactions of LFA-1 and Mac-1 with intercellular adhesion molecule-1 in facilitating adherence and transendothelial migration of human neutrophils in vitro, J. Clin. Invest. 83 (6) (1989) 2008–2017, https://doi.org/10.1172/JCI114111.
[106] M.S. Diamond, D.E. Staunton, A.R. de Fougerolles, S.A. Stacker, J. Garcia-Aguilar, M.L. Hibbs, T.A. Springer, ICAM-1 (CD54): a counter-receptor for Mac-1 (CD11b/CD18), J. Cell Biol. 111 (6 Pt 2) (1990) 3129–3139, https://doi.org/10.1083/jcb.111.6.3129.
[107] R. Gorina, R. Lyck, D. Vestweber, B. Engelhardt, beta2 integrin-mediated crawling on endothelial ICAM-1 and ICAM-2 is a prerequisite for transcellular neutrophil diapedesis across the inflamed blood-brain barrier, J. Immunol. 192 (1) (2014) 324–337, https://doi.org/10.4049/jimmunol.1300858.
[108] K. Ley, C. Laudanna, M.I. Cybulsky, S. Nourshargh, Getting to the site of inflammation: the leukocyte adhesion cascade updated, Nat. Rev. Immunol. 7 (9) (2007) 678–689, https://doi.org/10.1038/nri2156.
[109] O. Arslan, H. Akan, M. Arat, K. Dalva, M. Ozcan, G. Gürman, O. Ilhan, N. Konuk, M. Beksaç, A. Uysal, et al., Soluble adhesion molecules (sICAM-1, sL-Selectin, sE-Selectin, sCD44) in healthy allogenic peripheral stem-cell donors primed with recombinant G-CSF, Cytotherapy 2 (4) (2000) 259–265.
[110] L. Håkansson, M. Höglund, U.B. Jönsson, I. Torsteinsdottir, X. Xu, P. Venge, Effects of in vivo administration of G-CSF on neutrophil and eosinophil adhesion, Br. J. Haematol. 98 (3) (1997) 603–611.
[111] L.D. Greller, F.L. Tobin, Detecting selective expression of genes and proteins, Genome Res. 9 (3) (1999) 282–296.
[112] P.M. Bath, N. Sprigg, T. England, Colony stimulating factors (including erythropoietin, granulocyte colony stimulating factor and analogues) for stroke, Cochrane Database Syst. Rev. (6) (2013) CD005207, , https://doi.org/10.1002/14651858.CD005207.pub4.
[113] X. Huang, Y. Liu, S. Bai, L. Peng, B. Zhang, H. Lu, Granulocyte colony stimulating factor therapy for stroke: a pairwise meta-analysis of randomized controlled trial, PLoS One 12 (4) (2017) e0175774, , https://doi.org/10.1371/journal.pone.0175774.
[114] S. Ito, T. Uchida, N. Oshima, T. Oda, H. Kumagai, Development of membranoproliferative glomerulonephritis-like glomerulopathy in a patient with neutrophilia resulting from endogenous granulocyte-colony stimulating factor overproduction: a case report, BMC Nephrol. 19 (1) (2018) 251, https://doi.org/10.1186/s12882-018-1049-4.
[115] A. Martins, J. Han, S.O. Kim, The multifaceted effects of granulocyte colony-stimulating factor in immunomodulation and potential roles in intestinal immune homeostasis, IUBMB Life 62 (8) (2010) 611–617, https://doi.org/10.1002/iub.361.